Analysis of Wind-Driven and Water-Driven Transportation of Gross Solids in Urban Watersheds

Natalie Narváez

Submitted under the supervision of Dr. John Chapman to the University Honors Program at the University of Minnesota-Twin Cities in partial fulfillment of the requirements for the degree of Bachelor of Individualized Studies, *summa cum laude* in Psychology, Environmental Science, Policy & Management, and Earth Science.

December 18th, 2023

Acknowledgments

I would like to thank Dr. John Chapman, Dr. Jacques Finlay, and Dr. Grace Wilson for mentoring and advising me throughout this process, and Kathryn Hoffman, Aaron Pietsch, and Dr. Larry Baker for their guidance. I would also like to thank Rose Coyne, Brea Fahrner, Isabella Fischer, Marie Ronnander, and Makenna Tosi for their help with the detailed plant identification effort for the Pascal Center rain garden samples, and Dr. Erin Cortus and Dr. Sujaya Rao for allowing me to utilize their lab spaces and equipment for data collection.

Abstract

Watershed health is heavily influenced by urbanization and the export of associated pollutants such as nitrogen (N) and phosphorus (P) that leach into stormwater and accelerate the effects of eutrophication. In urban watersheds, gross solids materials have been shown to contribute significant amounts of P to stormwater runoff. Positive correlations have been identified between precipitation patterns and influxes of gross solids to stormwater runoff. However, the role of wind-driven transportation as a contributor of organic material to urban stormwater solids remains poorly understood in comparison to the role of water-driven transportation. Wind-blown leaf litter has the potential to travel beyond the hydrologically connected areas that bound much of the research on stormwater solids. To address this knowledge gap, a detailed analysis was conducted on identifiable tree material from gross solids samples captured at two different rain garden sites - one parking lot site and one residential street site - with low canopy cover in the Minneapolis-Saint Paul metropolitan region in Minnesota, USA, to assess the possible mechanisms behind their deposition into the rain garden sites. It was assumed that material from outside of the watershed was transported by wind. Findings showed that material from outside the hydrologic watershed plays a significant role in the prevalence of gross solids, with an average percentage of 29% of material from outside the watershed and 71% from inside the watershed. Material from outside the watershed represented the majority of identified material from the residential street site. Material from within the watershed appeared to rise and fall along with precipitation patterns while material from outside the watershed appeared to fluctuate opposite them, suggesting that material from outside the watershed is more dominant in dryer conditions. Results of this study suggest that material from outside the

watersheds represents a significant portion of leaf litter and other plant materials that constitute the organic fraction of urban stormwater solids.

1. Introduction & Background

Watershed health is heavily influenced by urbanization and the export of associated pollutants. When excessive amounts of mineral nutrients such as nitrogen (N) and phosphorus (P) leach into stormwater, they can cause damage to receiving waters by accelerating the effects of eutrophication, causing excessive production of autotrophs like algae and cyanobacteria which leads to oxygen depletion and the loss of aquatic animals (Selbig, 2016; Settle et al., 2017; Correll, 1998). Both anthropogenic (fertilizers, detergents, pet waste) and biogenic (leaves, seeds, grass clipping, pollen) sources of nutrient pollutants are of concern in areas where increased amounts of impervious surfaces have altered the hydrologic cycle, allowing pollutants to migrate directly from their source to receiving waters (Selbig, 2016; Rio et al., 2021; Winston et al., 2023). In urban areas with high overhead canopy cover, such as commercial and residential streets, biogenic sources of nutrient pollution have been shown to contribute significant amounts of P to urban stormwater runoff (Hobbie et al., 2014; Hobbie et al., 2017; Janke et al., 2017; Yang and Toor, 2017; Winston et al., 2023). Positive correlations have been identified between precipitation patterns and fluxes of biogenic sources of nutrient pollutants conveyed in urban stormwater runoff (Waickowski, 2015; Winston and Hunt, 2017; Chowdry et al., 2023; Winston et al., 2023). As a nutrient pollutant management strategy, street sweeping programs have been shown to significantly reduce the amount of P leached from organic debris during and after rainfall events by decreasing the amount of leaf litter and other organic gross solids conveyed in surface runoff (Selbig, 2016). However, the role of wind-driven transportation as a contributor of organic material to urban stormwater solids remains poorly understood in comparison to the role of water-driven transportation. Wind-blown leaf litter has the potential to travel beyond the hydrologically connected areas that bound much of the research on stormwater solids. Data are

needed to assess the contributions of wind-driven and water-driven transportation in the distribution of leaf litter and other plant materials that constitute significant portions of urban stormwater solids.

The objective of this study was to assess the possible mechanisms behind the deposition of material into the rain garden sites by analyzing the identifiable tree material from gross solids samples captured at two different rain garden sites with low canopy cover in the Minneapolis-Saint Paul metropolitan region in Minnesota, USA. In this study, water-transported material was operationally defined as material from tree species with instances where the canopy cover partially or completely overlapped the areas that were hydrologically connected to the sites such that stormwater flows from rain events could transport their dropped material into the rain gardens. Wind-transported material was operationally identified as material from tree species that were not present to any extent within the areas hydrologically connected to the sites, such that water transport could not account for the entirety of its deposition into the area hydrologically connected to the rain garden. For tree species without instances located within the areas hydrologically connected to the rain garden sites, the identified material was conservatively assumed to have originated from the nearest occurrence of that species to the rain garden.

2. Methods

2.1 Initial Sampling

Two rain garden sites with low canopy cover were selected from the 13 stormwater sites, where gross solids transport was studied in 2021 and 2022 as part of a research study. These sites were a rain guardian turret at the “Ski-U-Mah” Parking Lot (RG-2) located within a light commercial area on the University of Minnesota’s East Bank campus in Minneapolis with 16% canopy cover, and a curb-cut inlet to a rain garden (RG-6) in a residential street in Saint Paul’s

Como neighborhood with 1% canopy cover. Both sites had catchment basins installed to collect gross solids samples. At RG-2, the basin consisted of a mesh bag attached to a frame within the rain guardian turret. At RG-6, the basin consisted of a mesh bag attached to a small plastic inlet frame that followed the slope of the rain garden. The mesh fruit tree bags (70 by 48 cm) collected solids with diameters larger than approximately 2 mm that flowed in while allowing stormwater to drain out into the rain garden. Gross solids materials were collected from these sites at approximately 2-week intervals throughout the 2021 and 2022 sampling seasons, and after analysis, homogenized portions of each sample were dated and frozen for future use. In 2021, samples from the Task 3 sites were collected on 18 occasions, beginning on April 7th and concluding on the 1st of December.

Boulevard tree planting information was obtained for both sites, containing species identifications and planting locations. Planting information for the RG-2 site was provided by the University of Minnesota's Facilities Management Landcare team through the University of Minnesota Enterprise GIS Twin Cities campus *Trees by Type* data. This data set includes UMN-owned and non-UMN-owned trees planted on or near UMN property. Field reconnaissance was conducted to verify the UMN Landcare data and to identify and note the location of any trees near RG-2 that were not included in the *Trees by Type* data. The iNaturalist and Seek apps (https://www.inaturalist.org) were used to identify tree species in the field, and photos were cross-referenced with tree identification guides (Watts, 1963; Dirr, 2009). Boulevard tree planting information for the RG-6 site was provided by Daniel Anderson, an urban forester with the City of Saint Paul's Department of Parks & Recreation. This data, which included a spreadsheet and an ArcGIS shapefile, was specific to the street addresses provided in the data request and included only boulevard tree information. Field reconnaissance was conducted to

identify and note the location of trees near RG-6 that were not included in the boulevard planting data, including privately owned trees. The iNaturalist and Seek apps were used to identify tree species in the field, and photos were cross-referenced with tree identification guides (Watts, 1963; Dirr, 2009).

In June of 2022, all 14 available samples collected at the RG-2 site in 2021 were obtained from freezer storage, spanning collection dates from April 7th to December 1st, 2021, and allowed to thaw. Of the four sampling dates that were missing from the samples recovered from frozen storage, two had been lost before collection (May 20th and May 26th, 2021) due to a malfunction of the catchment basins in which the mesh sampler bags detached from the frame, causing all contents to be lost, and two had been discarded due to grease dumps (September 29th and November 9th, 2021) which skewed their mass and nutrient data.

In the fall of 2022, all 15 available samples collected at the RG-6 site in 2021 were obtained from freezer storage, spanning collection dates from April 30th to December 1st, 2021, and allowed to thaw. Of the three sampling dates that were missing from the samples recovered from frozen storage, a sample was never collected from the site on April 7th, 2021, and the samples collected on June 3rd and June 23rd, 2021 could not be located.

2.2 Detailed Plant ID and Sieve

A detailed plant identification analysis was performed on the RG-2 samples in August 2022. Samples were sorted one at a time, with their full contents emptied into a clean plastic bin and identified by species and plant part (leaves, seeds, flowers, flowers and seeds, fruit, and twigs). To aid in the identification process, a database was created with leaf, seed, and other identifiable plant part characteristics for each tree species in the area surrounding RG-2 as noted in the UMN Landcare data, along with any that were identified through field reconnaissance. The

iNaturalist and Seek apps were also used to aid tree species identification, and samples were cross-referenced with tree identification guides as needed (Watts, 1963; Dirr, 2009). The total mass of each identifiable plant part for each identifiable species was recorded in grams. All unidentifiable material was shaken manually for 60 seconds in a 1.68 mm sieve and the mass of the finer and coarser portions were recorded in grams.

A detailed plant identification analysis was performed on the RG-6 samples beginning in November of 2022 and concluding in April of 2023. This analysis was conducted with the help of five additional researchers: Rose Coyne, Brea Fahrner, Isabella Fischer, Kathryn Hoffman, Marie Ronnander, and Makenna Tosi. Samples were sorted one at a time, their full contents being emptied into a clean plastic bin and categorized by hand into species identifications (along with variety identifications when applicable), and plant part identifications (leaves, seeds, flowers, flowers and seeds, fruit, and twigs). To aid in the identification process, an additional Google Slides presentation was created with leaf, seed, and other identifiable plant part characteristics for each tree species in the area surrounding RG-6 as noted in the City of Saint Paul's boulevard planting data, along with additional species on residential property that were identified through field reconnaissance. The iNaturalist and Seek apps were used to aid tree species identification, and samples were cross-referenced with tree identification guides as needed (Watts, 1963; Dirr, 2009). After the identification process was completed for all available RG-6 samples from 2021, each identifiable plant part for each identifiable species was oven-dried to remove excess moisture prior to recording their masses. In preparation for the oven-drying the samples, a 6 lb or 2 lb AJM-brand paper bag (depending on the size of the identified portion) was labeled for every identified species and variety of plant part before being oven-dried at 105°C for a minimum of 48 hours and then stored in a desiccator at room

temperature. This was done to reduce the amount of interference to the recorded mass of each species/variety plant part due to moisture in the paper bags. When samples were ready to be oven-dried, the weight of each paper bag was recorded in grams before and after its sample was added. Filled paper bags were then oven-dried at 105°C for a minimum of 72 hours. Upon removal from the oven, the weight of each bag was recorded in grams and the dry mass of each portion was obtained by subtracting the initial weight of the oven-dried and desiccated empty paper bag from the final weight of the oven-dried and desiccated filled paper bag. All unidentifiable material was also oven-dried following the same process as the identified material before then being shaken mechanically for 60 seconds in a sieve stack with mesh sizes of 1.68 mm, 1 mm, 0.595 mm, 0.42 mm, and 0.177 mm. The mass of material collected in each sieve was recorded in grams.

2.3 Assessment of Hydrologic Connectivity and Mapping

Field reconnaissance was conducted at both rain garden sites during rain events to determine the areas hydrologically connected to them. These areas were any from which precipitation flowed into the respective rain garden, thus denoting where water-driven transportation of gross solids into each site could occur. Maps were created for both rain garden sites in ArcGIS Pro and the areas hydrologically connected to each were added as polygons. Each tree in the areas surrounding the rain gardens, as bounded by the acquired planting data and limitations of field reconnaissance efforts, was added to the map as a point, its location determined by the data provided by the Landcare Team, the City of Saint Paul, field reconnaissance. The species (and variety if applicable) of each tree was added manually to a data field that was created in the attribute table for the feature class. The rain gardens were added as points in a separate feature class. The distance between the trunk of each tree and the catchment

basin of the respective rain garden was calculated in meters using the Near (Analysis) geoprocessing tool from the ArcGIS Pro Proximity toolset. Geodetic lines were drawn to connect the nearest instance of each tree species to its respective rain garden using the Distance and Direction tool, thus providing the angles at which each nearest instance tree is located from its rain garden in degrees.

2.4 Precipitation and Wind Data

Precipitation data for the 2021 sampling season was obtained from the Minnesota Department of Natural Resources using their Daily Data custom climate summaries tool. Precipitation data recorded from the University of Minnesota's Saint Paul Campus Climate Observatory was the most representative of conditions at the Pascal Center rain garden (RG-6), and precipitation data recorded from the Minneapolis Saint Paul International Airport was the most representative of conditions at the Ski-U-Mah parking lot rain garden (RG-2). Wind data for the 2021 sampling season was obtained from Iowa State University's Environmental Mesonet custom Wind Rose tool (https://www.mesonet.agron.iastate.edu). Wind data recorded from the Minneapolis Saint Paul International Airport was the most representative of conditions at both rain garden sites. Wind data from the Saint Paul Downtown Airport was not used for the Pascal Center rain garden due to the climate station's proximity to the Mississippi River and the probable influence that the river valley has on local winds.

3. Results

3.1 Maps & Tables

3.1.1 RG-2

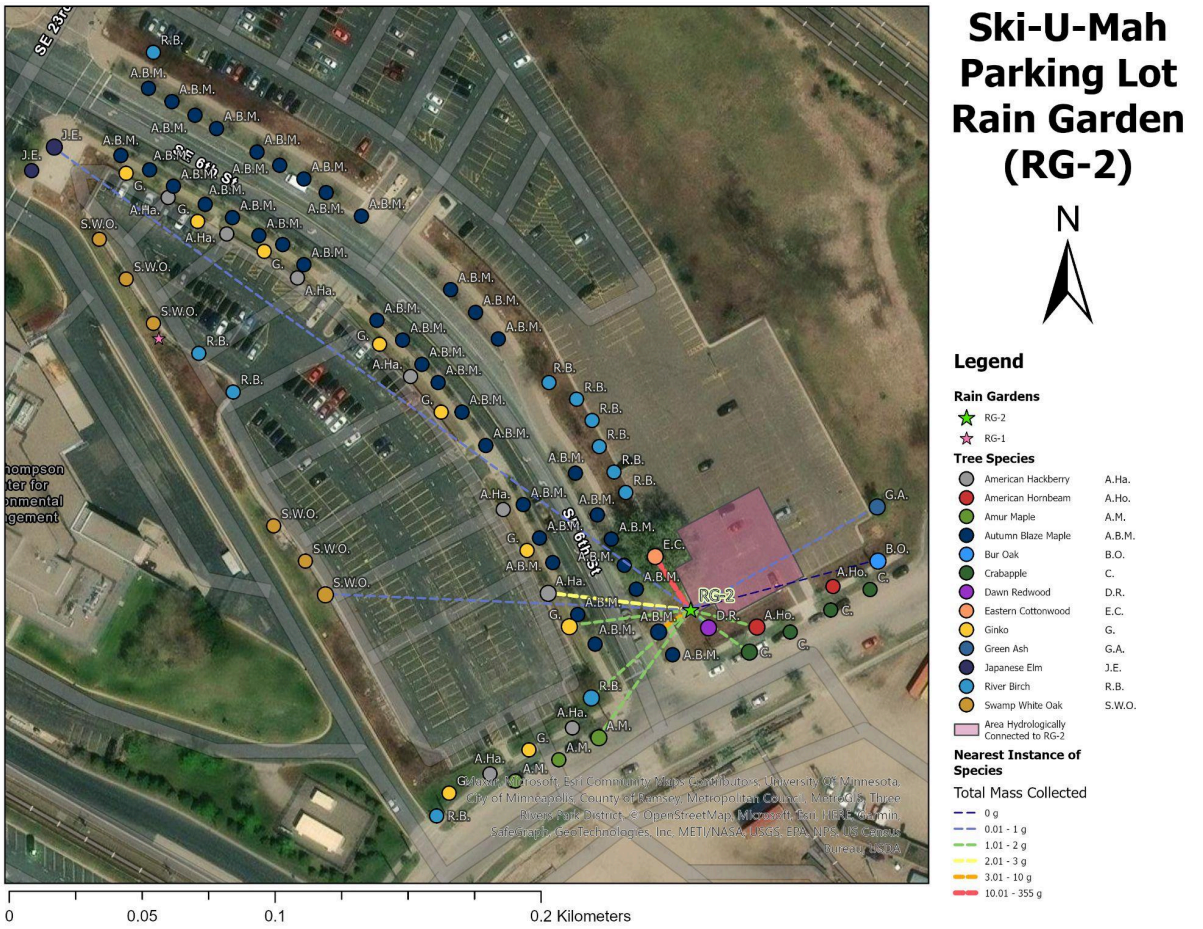

Figure 1. An aerial map of the RG-2 site displays nearby trees, differentiated by species, as noted in Landcare data and confirmed through field reconnaissance. The area hydrologically connected to RG-2 is represented by a shaded polygon. Geodetic lines connect RG-2 to the nearest instance of each tree species in the area and their coloring and width denote the range of the total mass collected from that species observed across the 2021 samples, with warmer colors and thicker lines representing higher amounts of total mass collected.

Table 1. Tree species data from the area surrounding the RG-2 site - organized by the total mass of material found per species - including the distance to the nearest instance of each species, whether the species was identified in the 2021 samples, the angle from the RG-2 catchment basin to the trunk of the nearest instance, whether the nearest instance was located on a boulevard, the number of recorded instances in the area surrounding the rain garden, and whether or not an instance of the species was located partially or entirely within the area hydrologically connected to the rain garden.

Tree Species Information from the Ski-U-Mah Parking Lot Rain Garden Site (RG-2) in 2021						
Tree Species Common Name (*Scientific Name*)	**Total Species Mass Collected in 2021 Samples (g)**	**Distance to Nearest Instance (m)**	**Species Found Within Samples (Yes (*Y*) or No (*N*))**	**Angle to Nearest Instance (°)**	**Location of Nearest Instance (Boulevard (*B*) or Yard (*Y*))**	**# of Recorded Instances**
Eastern Cottonwood* *(Populus deltoides)*	*354.25*	*23.93*	*Y*	*326.55*	*Y*	*1*
Autumn Blaze Maple *(Acer freemanii)*	*8.35*	*14.72*	*Y*	*237.47*	*B*	*38*
American Hackberry *(Celtis occidentalis)*	*2.85*	*54.02*	*Y*	*276.84*	*Y*	*8*
Crabapple *(Malus)*	*1.75*	*27.20*	*Y*	*125.33*	*B*	*4*
River Birch *(Betula nigra)*	*1.65*	*49.98*	*Y*	*228.32*	*Y*	*11*
American Hornbeam *(Carpinus caroliniana)*	*1.20*	*25.70*	*Y*	*104.25*	*Y*	*2*
Amur Maple *(Acer ginnala)*	*1.15*	*59.25*	*Y*	*215.91*	*B*	*3*
Ginko *(Ginkgo biloba)*	*1.10*	*46.16*	*Y*	*262.59*	*Y*	*9*
Green Ash *(Fraxinus pennsylvanica)*	*0.20*	*80.07*	*Y*	*61.30*	*Y*	*1*
Japanese Elm *(Ulmus davidiana var. japonica)*	*0.20*	*295.62*	*Y*	*305.80*	*B*	*2*
Swamp White Oak *(Quercus bicolor)*	*0.20*	*137.47*	*Y*	*272.47*	*Y*	*4*
Dawn Redwood *(Metasequoia)*	*0.05*	*9.56*	*Y*	*132.78*	*Y*	*1*
Bur Oak *(Quercus macrocarpa)*	*0.00*	*72.70*	*N*	*75.17*	*Y*	*1*
** Denotes species with instances partially or entirely within the area hydrologically connected to the rain garden*						

At the Ski-U-Mah Parking Lot rain garden site, 12 of the 13 nearby tree species were identified within the 2021 samples. The nearby species that was not identified was the Bur Oak, located just over 70 meters northeast of the rain garden. The nearest instance of Green Ash was located farther northeast of RG-2, but its canopy overhangs a portion of the parking lot whereas the Bur Oak is located entirely outside of it. Although it was not the closest tree to the rain garden, the Eastern Cottonwood was the only species in the area located within the area

hydrologically connected to the rain garden due to its canopy cover partially overlapping it. Its large canopy overhangs a portion of the Ski-U-Mah parking lot that slopes towards RG-2 (Figure 1), increasing the likelihood that its fallen plant material in that area would be carried by stormwater flows toward the rain garden. The Japanese Elm was the species with the most distant nearest instance to appear in the samples, located over 295 meters northwest of RG-2.

3.1.2 RG-6

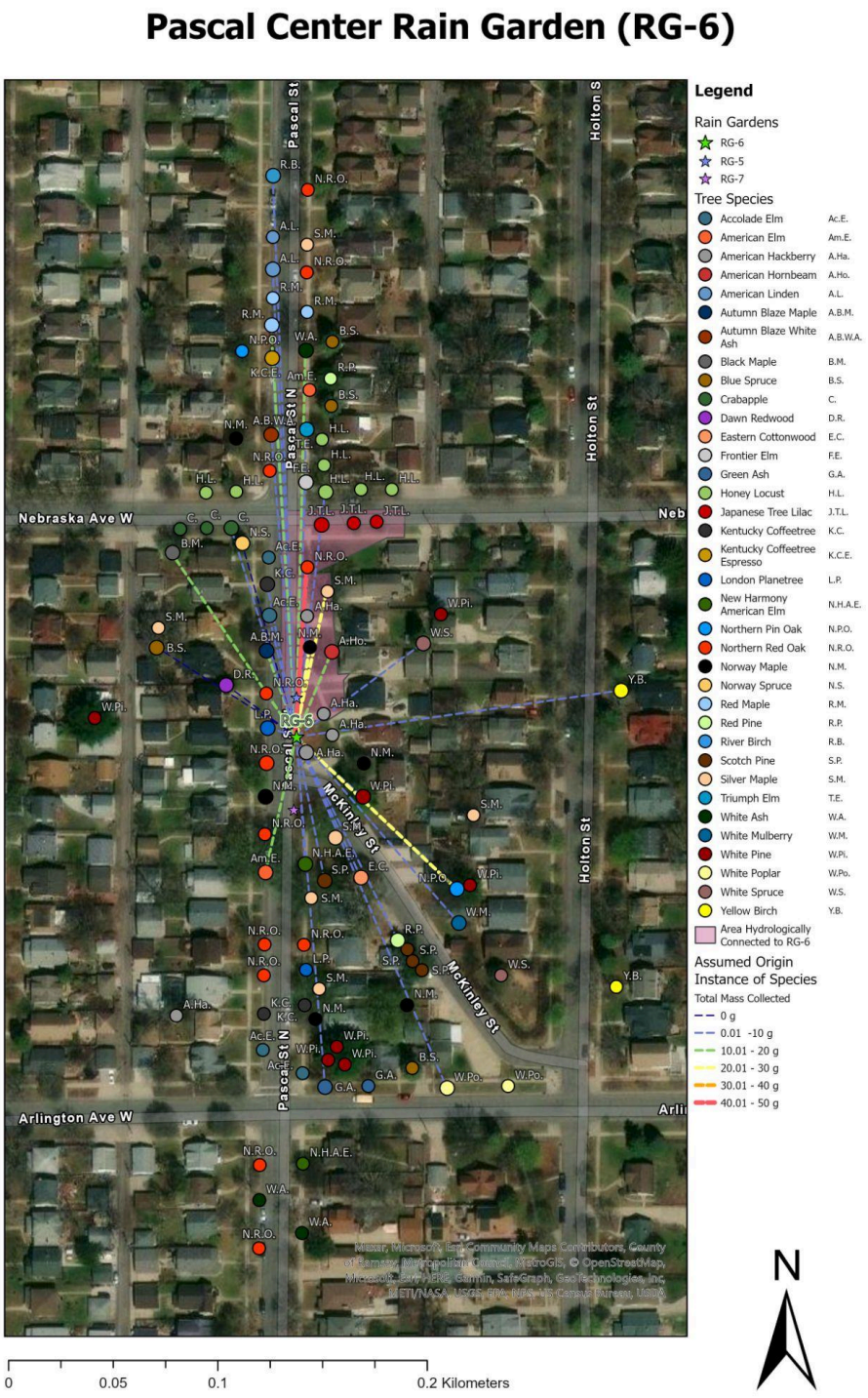

Figure 2. An aerial map of the RG-6 site displays nearby trees, differentiated by species, as noted in Landcare data and confirmed through field reconnaissance. The area hydrologically connected to RG-6 is represented by a shaded polygon. Geodetic lines connect RG-2 to the nearest instance of each tree species in the area and their coloring and width denote the range

of the total mass collected from that species observed across the 2021 samples, with warmer colors and thicker lines representing higher amounts of total mass collected.

Table 2. Tree species data from the area surrounding the RG-6 site - organized by the total mass of material found per species - including the distance to the nearest instance of each species, whether the species was identified in the 2021 samples, the angle from the RG-6 catchment basin to the trunk of the nearest instance, whether the nearest instance was located on a boulevard, the number of recorded instances in the area surrounding the rain garden, and whether or not an instance of the species was located partially or entirely within the area hydrologically connected to the rain garden.

Tree Species Information from the Pascal Center Rain Garden Site (RG-6) in 2021						
Tree Species Common Name (*Scientific Name*)	**Total Species Mass Collected in 2021 Samples (*g*)**	**Distance to Nearest Instance (m)**	**Species Found Within Samples (Yes (*Y*) or No (*N*))**	**Angle to Nearest Instance (°)**	**Location of Nearest Instance (Boulevard (*B*) or Yard (*Y*))**	**# of Recorded Instances**
Northern Red Oak* *(Quercus rubra)*	*49.53*	*13.51*	*Y*	*3.86*	*B*	*12*
Norway Maple* *(Acer platanoides)*	*27.41*	*22.78*	*Y*	*8.16*	*B*	*6*
Silver Maple* *(Acer saccharinum)*	*24.42*	*36.36*	*Y*	*12.33*	*Y*	*7*
Northern Pin Oak *(Quercus ellipsoidalis)*	*21.12*	*74.62*	*Y*	*133.32*	*Y*	*2*
Autumn Blaze Maple *(Acer freemanii)*	*18.68*	*30.61*	*Y*	*340.42*	*B*	*1*
American Elm *(Ulmus americana)*	*18.35*	*46.76*	*Y*	*192.82*	*B*	*2*
White Ash *(Fraxinus americana)*	*16.30*	*130.06*	*Y*	*1.39*	*B*	*3*
American Hornbeam* *(Carpinus caroliniana)*	*11.80*	*30.97*	*Y*	*22.69*	*Y*	*1*
Black Maple *(Acer nigrum)*	*11.80*	*74.92*	*Y*	*325.75*	*Y*	*1*
Red Maple *(Acer rubrum)*	*10.23*	*138.73*	*Y*	*356.47*	*B*	*3*
New Harmony American Elm *(Ulmus americana 'New Harmony')*	*8.46*	*42.89*	*Y*	*176.43*	*B*	*2*
Accolade Elm *(Ulmus 'Morton')*	*5.99*	*41.92*	*Y*	*346.80*	*B*	*4*
Autumn Blaze White Ash *(Fraxinus americana 'Autumn Blaze')*	*4.99*	*102.05*	*Y*	*355.32*	*B*	*1*
Frontier Elm *(Ulmus 'Frontier')*	*3.66*	*85.74*	*Y*	*2.12*	*B*	*1*
American Hackberry* *(Celtis occidentalis)*	*3.50*	*6.18*	*Y*	*5.46*	*B*	*5*
Green Ash *(Fraxinus pennsylvanica)*	*3.34*	*118.19*	*Y*	*175.25*	*B*	*2*
Triumph Elm *(Ulmus 'Morton Glossy')*	*3.21*	*103.41*	*Y*	*1.93*	*B*	*1*
Yellow Birch *(Betula alleghaniensis)*	*2.91*	*110.96*	*Y*	*81.88*	*Y*	*2*

Eastern Cottonwood *(Populus deltoides)*	*1.53*	*52.14*	*Y*	*155.31*	*Y*	*1*
London Planetree *(Platanus × acerifolia)*	*1.27*	*10.2*	*Y*	*286.50*	*B*	*2*
White Poplar *(Populus alba)*	*0.99*	*128.65*	*Y*	*156.69*	*B*	*2*
Honey Locust *(Gleditsia triacanthos)*	*0.76*	*82.94*	*Y*	*6.77*	*B*	*7*
White Spruce *(Picea glauca)*	*0.47*	*53.13*	*Y*	*53.62*	*Y*	*2*
Kentucky Coffeetree Espresso *(Gymnocladus dioicus 'Espresso')*	*0.42*	*127.63*	*Y*	*356.30*	*B*	*1*
White Pine *(Pinus strobus)*	*0.31*	*30.24*	*Y*	*132.04*	*Y*	*7*
White Mulberry *(Morus alba)*	*0.23*	*83.37*	*Y*	*138.93*	*Y*	*1*
River Birch *(Betula nigra)*	*0.18*	*188.98*	*Y*	*357.60*	*B*	*1*
Red Pine *(Pinus resinosa)*	*0.17*	*76.54*	*Y*	*153.36*	*Y*	*2*
Kentucky Coffeetree *(Gymnocladus dioicus)*	*0.14*	*52.28*	*Y*	*349.11*	*B*	*3*
Crabapple *(Malus)*	*0.03*	*73.62*	*Y*	*342.49*	*B*	*3*
American Linden *(Tilia americana)*	*0.01*	*157.46*	*Y*	*357.12*	*B*	*2*
Scotch Pine *(Pinus sylvestris)*	*0.01*	*49.37*	*Y*	*168.77*	*Y*	*4*
Blue Spruce *(Picea pungens)*	*0.00*	*56.03*	*N*	*302.32*	*Y*	*4*
Dawn Redwood *(Metasequoia)*	*0.00*	*29.46*	*N*	*306.47*	*Y*	*1*
Japanese Tree Lilac* *(Syringa reticulata)*	*0.00*	*71.84*	*N*	*6.81*	*B*	*3*
Norway Spruce *(Picea abies)*	*0.00*	*67.64*	*N*	*344.28*	*Y*	*1*
** Denotes species with instances within the area hydrologically connected to the rain garden*						

At the Pascal Center rain garden site, 32 of 36 nearby tree species were identified within the 2021 samples. Of the 4 species not identified in the samples, the Japanese Tree Lilac was the only one located within the area hydrologically connected to the rain garden (Figure 2). The nearest instance of American Hackberry was the closest species to the site, but its 3 closest instances are all relatively young plantings with small canopies, and the species accounted for only 1% of the total identified mass across the 2021 samples. The Northern Red Oak accounted

for the greatest portion of the total identified mass, 20%, and although an instance of the species was located within the area hydrologically connected to RG-6, the nearest instance was located southwest of the site and outside of the hydrologically connected area. The American Linden was the species with the most distant nearest instance to appear in the samples, located at over 157 meters north of RG-6, and with only 0.01 grams (Table 2), it also accounted for the smallest portion of the identified species.

3.2 Prevalence of Identified Material from Species Within and Outside of the Hydrologically Connected Areas

a)

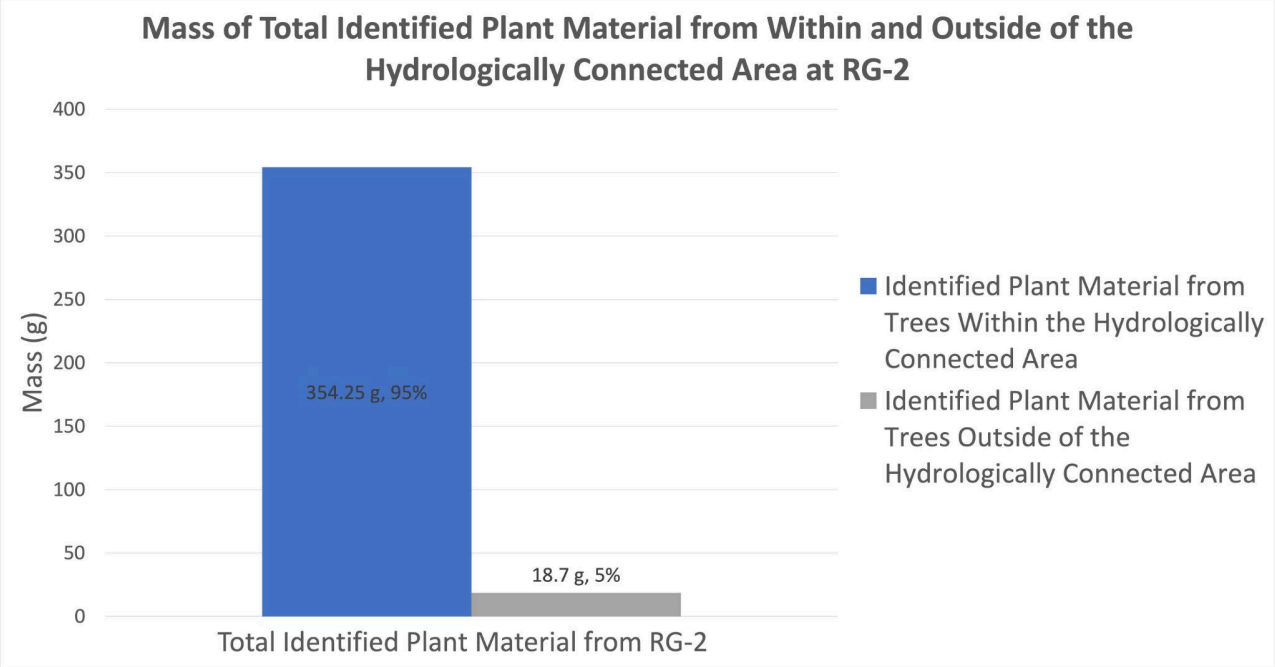

b)

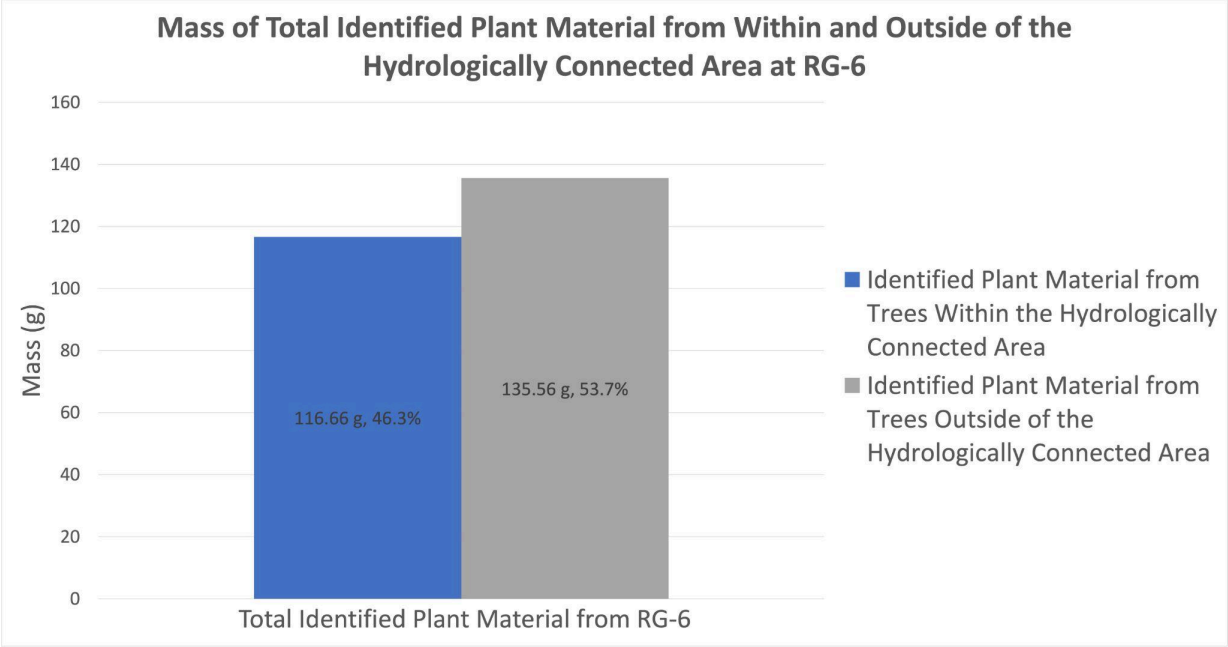

c)

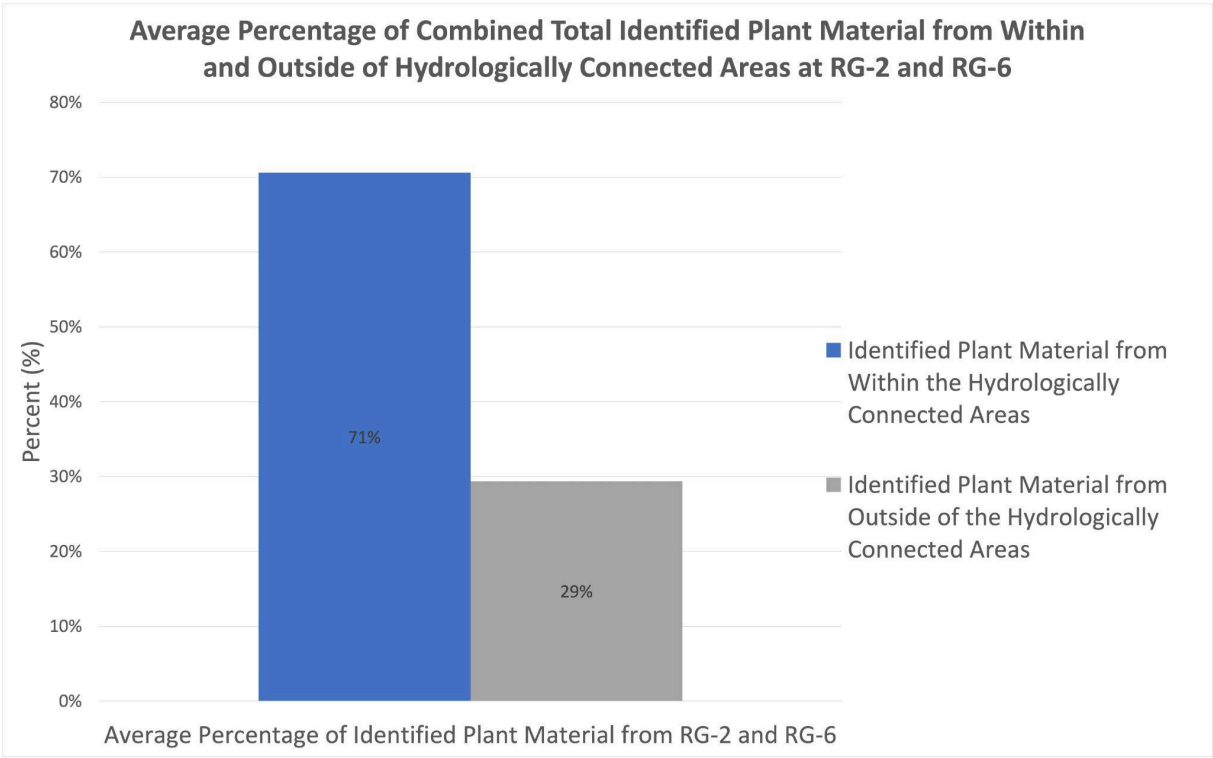

Figure 3. The combined mass of all identified material from species outside of the areas hydrologically connected to the rain garden compared to the combined mass of all identified material from species with instances within the hydrologically connected areas at RG-2 (a) and RG-6 (b). c) The average percentage of identified material from species outside of the areas hydrologically connected to both rain garden sites compared to the average percentage of all identified material from species with instances within the areas hydrologically connected to them based on the percentage of each at RG-2 and RG-6.

The percentage of total identified mass from species with instances within the areas hydrologically connected to the rain gardens compared to the total identified mass from species outside of the areas hydrologically connected differed considerably from RG-2 to RG-6 (Figure 3a and 3b). At RG-2, the mass of Eastern Cottonwood material, 354.25 grams (Table 1, Figure 3a), accounted for 95% of the total identified plant material in the 2021 samples, and the other 5% came from trees outside of the area hydrologically connected to RG-2. At RG-6, the total mass of identified plant material from species outside of the area hydrologically connected to the rain garden was greater (53.7%) than that of material from species with instances within the hydrologically connected areas (46.3%) (Figure 3b). The average percentage of material from species with instances within the areas hydrologically connected to the rain gardens (71%) is greater than that for material from species outside of the hydrologically connected areas (29%) (Figure 3c), but the difference is less extreme than what was observed across the RG-2 samples. Insight derived from Figure 3c may be inaccurate as this plot shows the average percentage of combined mass from two sites with different watershed areas, canopy cover, and tree species. While it would be preferable to normalize these two sites by a common parameter, I have not identified one at this time. Typically a normalization by watershed area would be used, but this data suggests that watershed area is not adequate for this purpose.

3.3 Cumulative Precipitation and Identified Mass from Species Within and Outside of the Hydrologically Connected Areas

a)

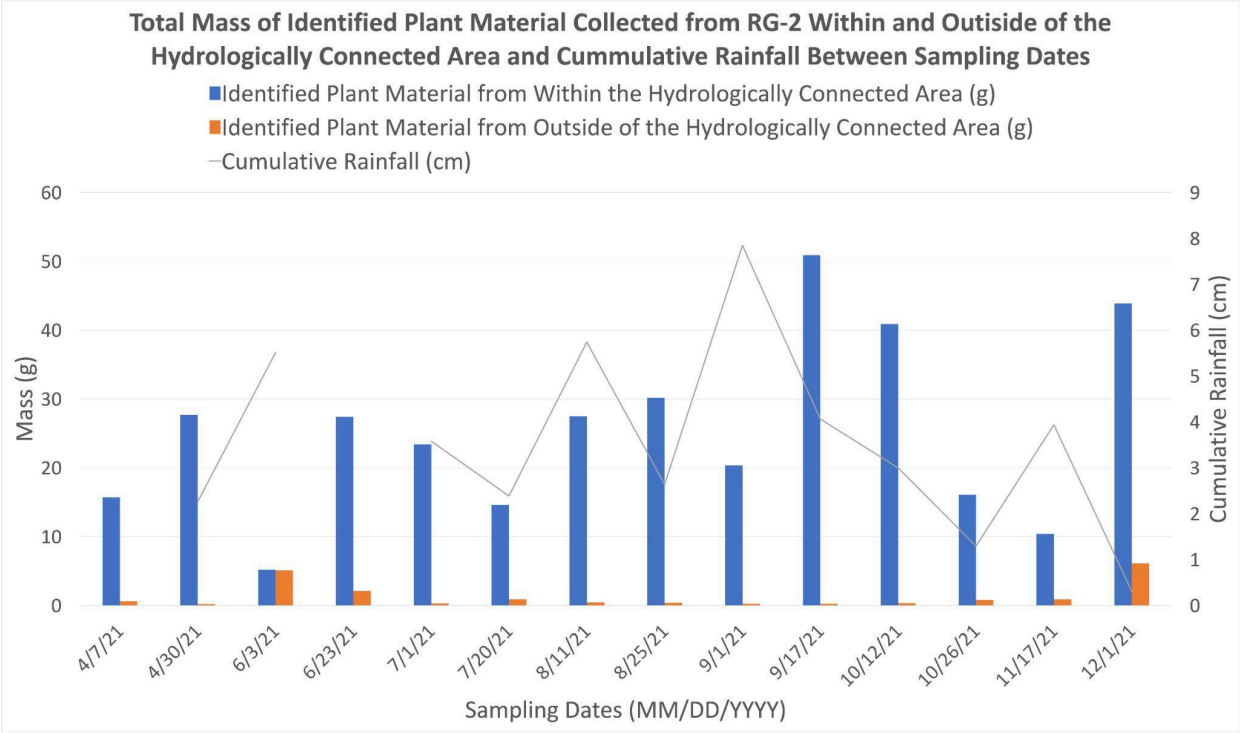

b)

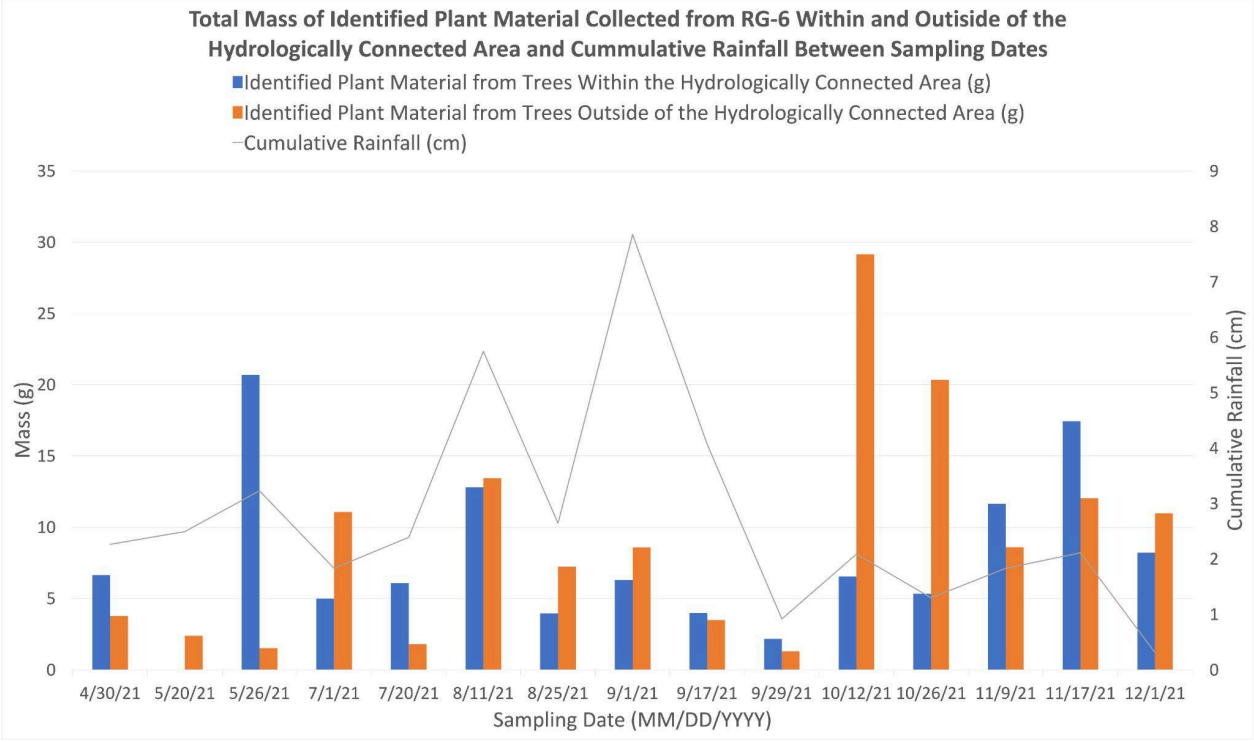

Figure 4. The combined mass of identified material from species outside of the areas hydrologically connected to the rain garden compared to the combined mass of identified material from species with instances within the hydrologically connected areas at RG-2 (a) and RG-6 (b) by sampling date, with cumulative precipitation between sampling dates plotted on a secondary axis.

The cumulative precipitation between sampling dates was identical for most sampling dates, but slightly higher for the RG-2 site than the RG-6 site over 3 sampling periods. The mass of material collected from both sites was the greatest in the fall (Figures 4a and 4b). Cumulative precipitation between sampling dates was highest in the summer and lowest at the end of fall. Across both sites, decreases in the amount of cumulative precipitation between sampling dates generally correlated with increases in the mass of identified material from species outside the hydrologically connected area, whereas increases in cumulative precipitation between sampling dates generally correlated with increases in the mass of identified material from species with instances within the areas hydrologically connected to each rain garden.

3.4 Cumulative Wind Data And Identified Mass Based on Angle to Nearest Instance

The wind roses in the following figures were created using Iowa State University's Environmental Mesonet Custom Wind Roses tool. They display the cumulative wind data collected from the Minneapolis Saint Paul International Airport over the 2021 sampling season based on compass directions and wind speed measurements from 5,907 observations made between the 30th of March and the 1st of December, 2021. The compass directions are divided into 36 bins which each span a different 10° range between 0° and 360°. Overlaid on the cumulative wind data is the cumulative mass of identified material based on the angle from the respective rain garden to the nearest instance of each species. The angles to the nearest instance of each species were matched with their corresponding compass direction bins, and the cumulative mass of identified material was calculated from all of the species within each of the 36 compass direction bins. The cumulative mass of identified material was then plotted on the

cumulative wind data, providing a visual representation of the relationship between the mass of identified material from each rain garden and the cumulative wind data from the 2021 sampling season.

a)

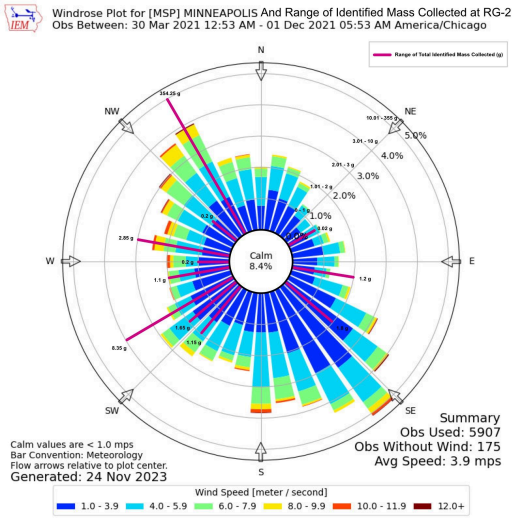

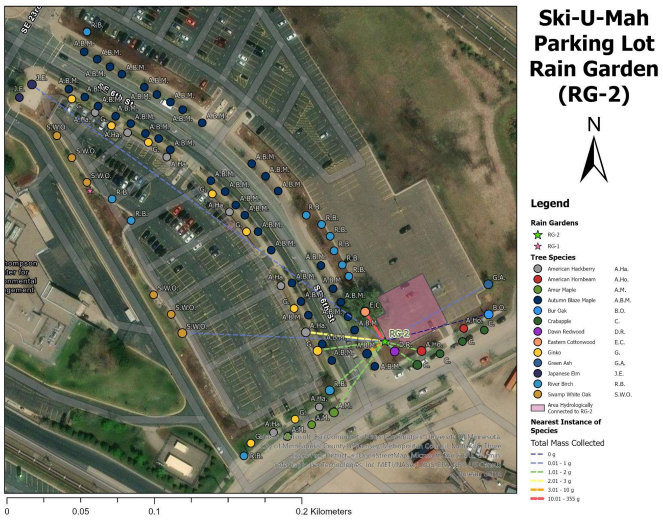

b)

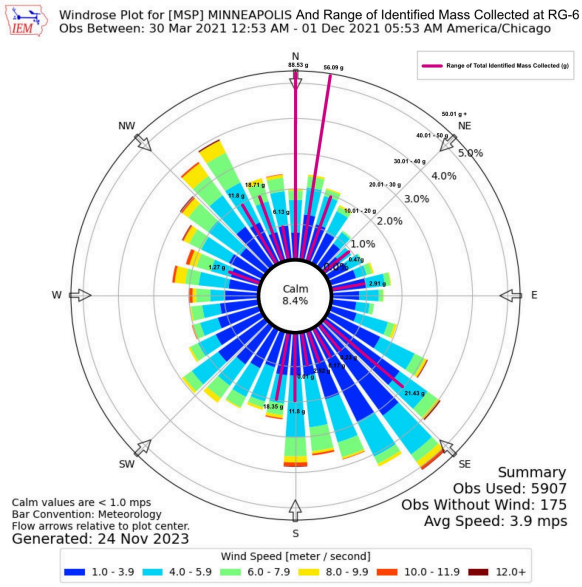

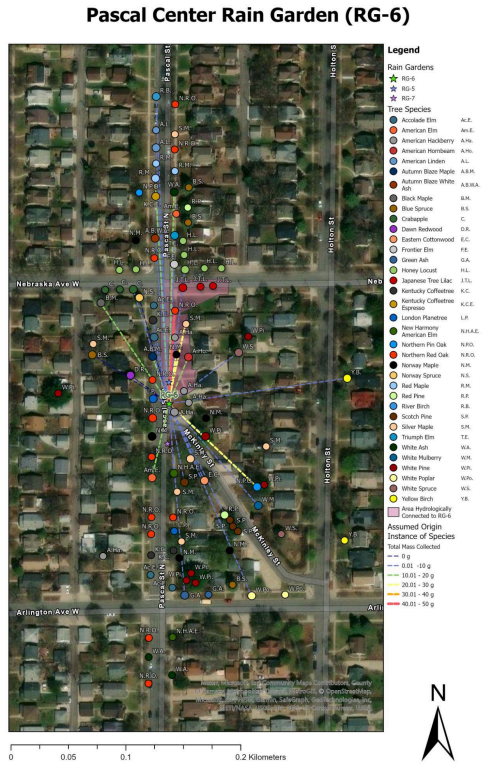

Figure 5. Cumulative wind data from March 30th through December 1st, 2021, overlaid with the range of cumulative mass of identified species based on the angle of their nearest instance from the respective rain garden, shown alongside the aerial map for the respective rain garden (RG-2 in a; RG-6 in b). Both wind rose figures utilize the same concentric axis circles for the wind data and the range of total identified mass collected, but the ranges of total identified mass collected differ for each. The wind data for both sites was sourced from the Minneapolis Saint Paul International Airport.

a)

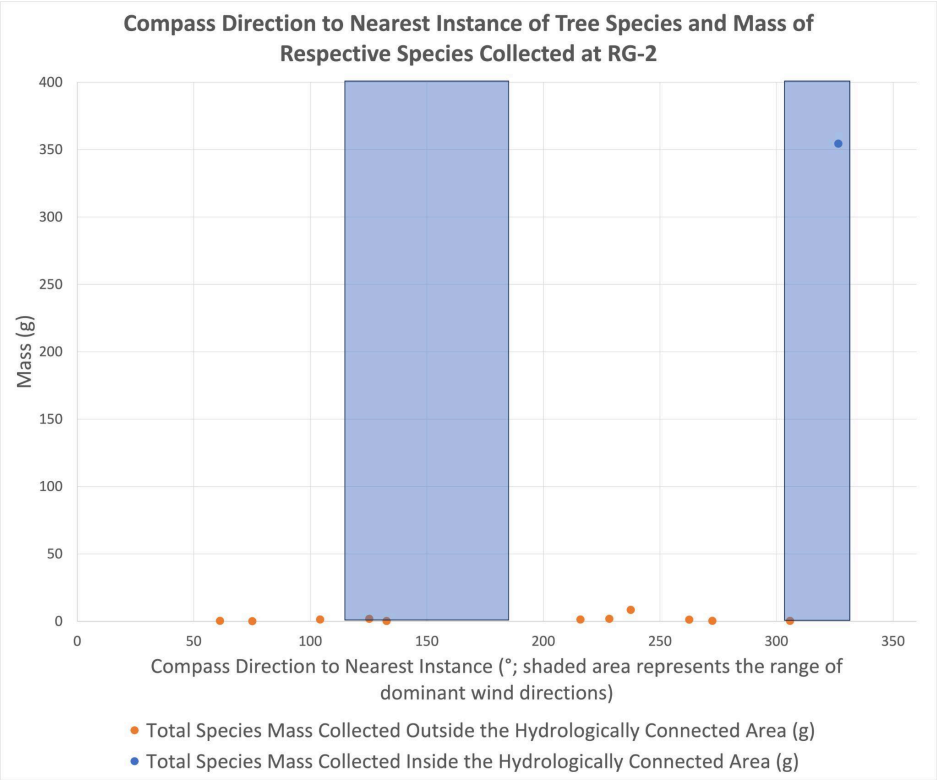

b)

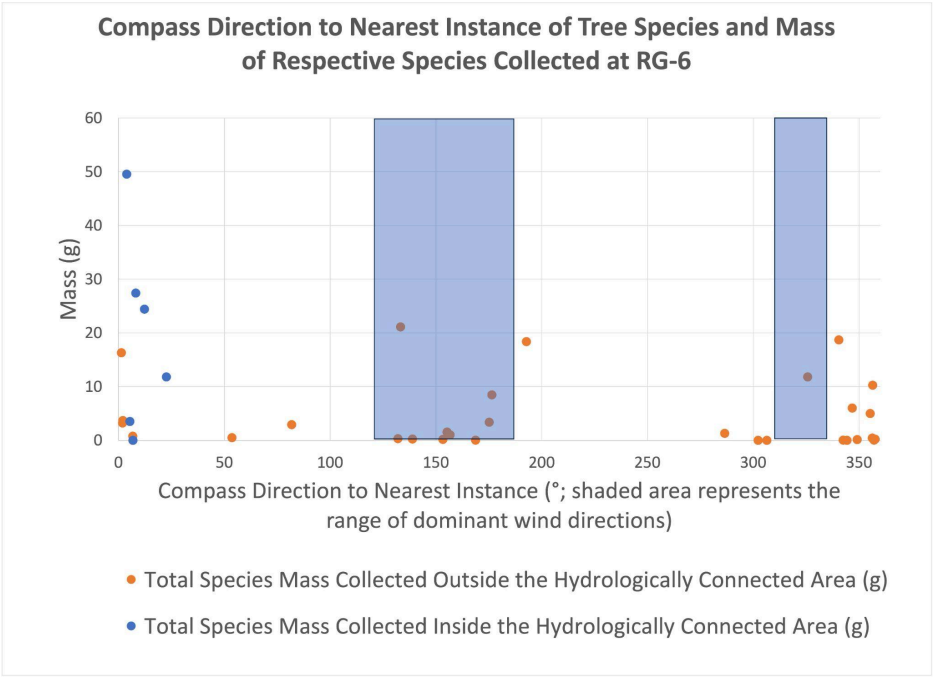

Figure 6. Scatterplots of compass directions from the catchment basin of the respective rain gardens (RG-2 in a; RG-6 in b) to the trunk of the nearest instance of tree species and the total mass collected for each species. Points are color-coded to denote whether the respective tree species was located within or outside of the area hydrologically connected to the rain garden. Shaded areas represent the range of dominant wind directions based on the 2021 data sourced from the Minneapolis Saint Paul International Airport between March 30th and December 1st, 2021.

At RG-2, the compass direction bin with the largest amount of cumulative mass, containing the Eastern Cottonwood tree with canopy overlapping the area hydrologically connected to the rain garden, is the range with the fourth-greatest cumulative winds in 2021 (325° - 334°), falling within the ranges of dominant wind directions based on the 2021 data (115° - 184° and 305° - 334°) (Figure 5a and Figure 6a). When compared with the aerial map of the area, the absence of mature trees located southeast of the rain garden can be noted as aligning with the two most dominant compass direction bins for wind in 2021 (135° - 144° and 145° - 154°). At RG-6 (Figure 5b), the two compass direction bins with the largest amounts of cumulative mass (355° - 004° and 005° - 014°) do not align with the ranges of dominant wind directions based on the 2021 data (115° - 184° and 305° - 334°), but both of them include portions of the hydrologically connected area. At RG-6, there appear to be clusters of mass collected from species outside the area hydrologically connected to the rain garden that align with the range of dominant wind directions. However, the three largest masses collected at RG-6 do not align with these ranges, suggesting that they were water-driven and aligning with their categorization as having originated from within the hydrologically connected area (Figure 6b). The mass collected at RG-2 does not follow the range of dominant wind directions as well as the mass collected at RG-6, but this may be explained by the closer proximity of trees located outside the area hydrologically connected to RG-2 reducing the wind speed required to transfer their material into the capture area (Figure 6a).

The species at RG-6 with the largest amount of identified mass, Northern Red Oak, has an instance within the area hydrologically connected to the rain garden that was defaulted to.

However, should the location of the second nearest instance of a Northern Red Oak tree - which is located northwest of RG-6 and outside of the area hydrologically connected to the rain garden - be utilized instead of the instance within the hydrologically connected area, that large amount of mass would instead fall into the same compass direction bin as the nearest instance of a black maple (335° - 344°), and the total mass collected from that bin would be 61.33 grams, making it the bin with the greatest gross solids contribution to RG-6. This is the same bin with the greatest gross solids contribution to RG-2 as it contains the Eastern Cottonwood tree, and it falls within the range of dominant wind directions in 2021.

The northwestern winds may have contributed additional gross solids material to RG-6 from trees located north of Nebraska Avenue West, such as the Autumn Blaze White Ash and the Red Maples on the western side of Pascal Street North, by blowing their leaves and seeds southeast, towards the area hydrologically connected to RG-6 (Figure 5b). The northwestern winds may have also reduced gross solids contributions to RG-6 from trees on the western side of Pascal Street North and south of Nebraska Avenue West by depositing them into the Pascal North (RG-5) and Pascal South (RG-7) rain gardens, located north and south of RG-6 respectively on the eastern side of Pascal Street North. The degree ranges with high amounts of cumulative identified mass also appear to display a general alignment with the streets surrounding both sites.

3.5 Distance to Nearest Instance Compared to Total Identified Mass

a)

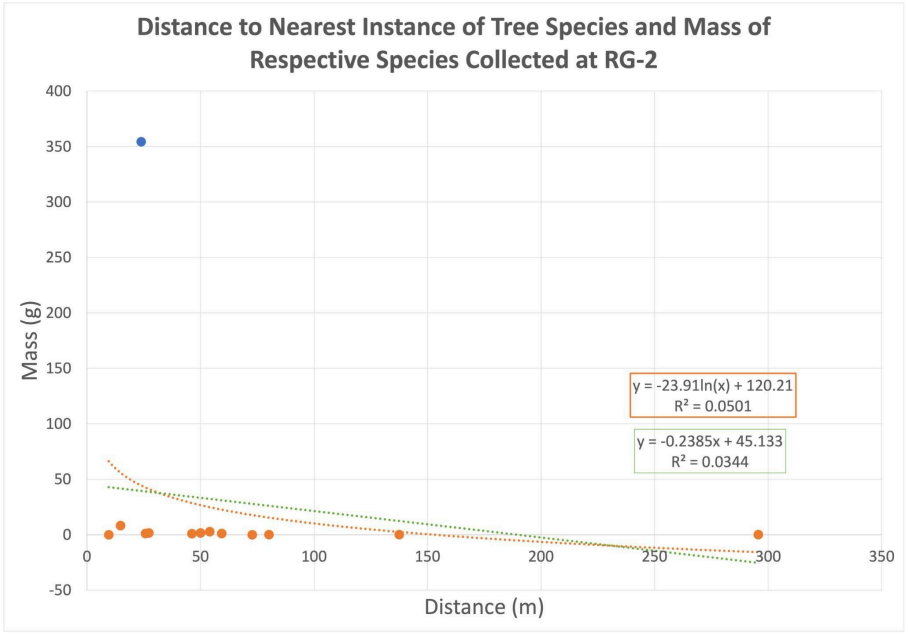

b)

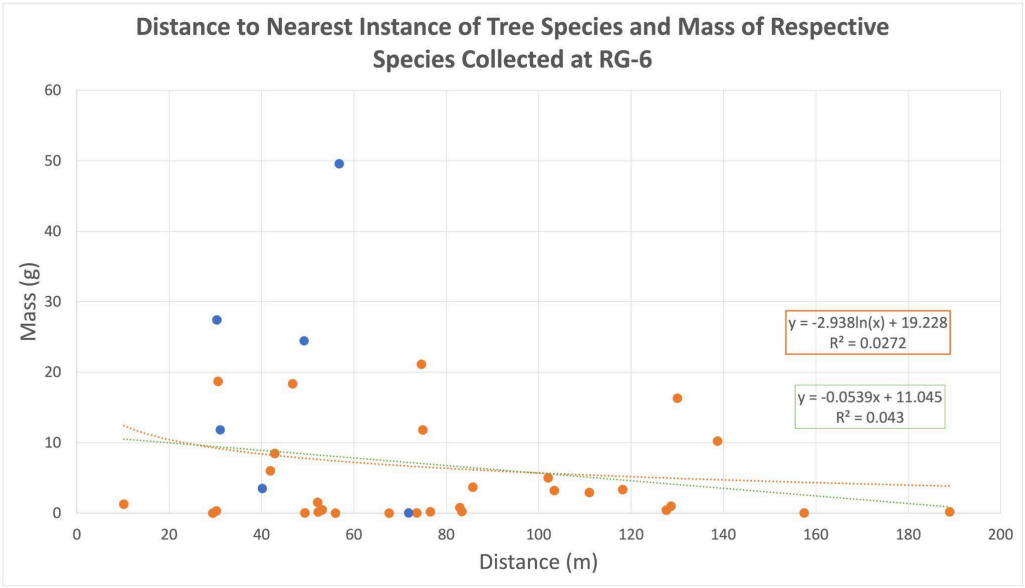

Figure 7. Scatterplot charts of distance from the respective catchment basin to the trunk of the nearest instance of each tree species and the total mass of identified material from that species across all 2021 samples analyzed from RG-2 (a) and RG-6 (b). Distances were calculated from the catchment basin of each rain garden to the trunk of the nearest instance of each tree species. Both scatterplots distinguish between species with instances within the area hydrologically connected to the respective rain garden, and they include logarithmic trendlines.

The R^2 values for the linear trendlines of distance from the respective catchment basin to the trunk of the nearest instance compared to the total identified mass were generally low for both sites (RG-2: $R^2 = 0.0344$; RG-6: $R^2 = 0.043$). Although the coefficients of determination remained generally low, the trend of the relationship at RG-2 of the distance to the nearest instance of each tree species and the total identified mass across all 2021 samples was better fit with logarithmic trendline whereas the trend of the same relationship at RG-6 was better fit by the linear trendline, as represented by the respective R^2 values for the linear trendlines (RG-2: $R^2 = 0.0501$; RG-6: $R^2 = 0.0272$) (Figure 7a and 7b). The assumption that identified material originated from the nearest instance of a respective species is likely to influence the strength of these relationships, potentially artificially inflating them compared to if the origin of mass could be determined with certainty.

4. Discussion

Based on the operational definitions of wind-driven and water-driven transport defined in the background of this study, Figure 3 - on the prevalence of identified material from species within and outside of the areas hydrologically connected to the rain gardens - shows that both wind-driven and water-driven transportation play significant roles in the transportation of gross solids. Material was identified at both sites from tree species outside of their hydrologically connected areas. Although the average percentage of identified material from species with instances within the hydrologically connected areas (71%) was greater than that of identified material from species outside of the hydrologically connected areas (29%), the identified

material from trees outside of the hydrologically connected area still accounted for over half of the identified material from RG-6, even with the mass from species with nearest instances outside of the hydrologically connected area included in the total mass of identified material from trees within the hydrologically connected area as long as any instance occurred within it. Water-driven transportation appeared to rise and fall along with trends in cumulative rainfall between sampling dates, whereas wind-driven transportation appeared to generally fluctuate opposite the trends in cumulative rainfall. These patterns suggest that wind-driven transportation is more dominant in dryer conditions, supporting the notion that drier, lighter leaves tend to be dispersed further from their source than their wetter and heavier counterparts (Ferguson, 1985). Increased leaf drop and reduced precipitation in the fall produce ideal conditions for increases in wind-driven transportation of gross solids. Residential fall street sweeping programs may be well suited to address a significant portion of this influx of material and prevent significant increases in nutrient pollution to urban water bodies, but the timing of these programs is of key importance. Sweeping before the majority of leaves have fallen, or before the wind has moved material into the streets could result in a lot of material being missed along with the resulting increases in nutrient pollution. A more detailed understanding of species that make up boulevard tree plantings, as well as their phenologies within local climates, could inform the timing of fall street sweeping programs and improve their impacts on nutrient loading to urban water bodies.

The significant differences in the water-transported and wind-transported portions of material collected at each site suggest that their locations and the use of land surrounding them could have measurable effects on the influence of different mechanisms behind the deposition of material into the rain garden sites. RG-2 is located in the southeastern corner of a parking lot within a light commercial area, whereas RG-6 is located on the eastern side of a north-south

street within a residential neighborhood. Larger cumulative masses were observed when the wind direction was aligned parallel to the street direction (Figures 5a and 5b), suggesting that the roads may have served as corridors along which local winds were accelerated due to fragmentation and local traffic, and where the curbs may have served as bumpers, channeling more material along the roadways, and even into the Pascal rain gardens due to their curb-cut design. The area surrounding RG-2 contains more impervious surfaces and less vegetation cover than RG-6, as well as fewer structures to contribute to the fragmentation of local winds, possibly facilitating the distribution of plant material across greater distances than at the RG-6 site, where the greatest distance to an identified species was 188.98 m (*Betula nigra*) compared to 295.62 m (*Ulmus davidiana var. japonica*) at RG-2 (Warneke et al., 2022). The Victory Parking Lot site (RG-1) was located far enough from RG-2 that it is unlikely to have impacted the number of species identified within the RG-2 samples. The increased amount of fragmentation in the area surrounding the RG-6 site due to residential housing may have led to a general deceleration of local winds, as well as to more redirection and acceleration along the orientation of the streets - primarily north-south - while reducing the speed of east-west winds (Damschen et al., 2014). Higher amounts of vegetation cover in the area surrounding RG-6 may also have reduced the influence of wind-driven transportation (Warneke et al., 2022). Additionally, the Pascal North (RG-) and Pascal South (RG-7) rain garden sites were accumulating material from the trees in the area during the same sampling periods as RG-6. They might contain different species that were not identified in the RG-6 samples, including material from the three Japanese Tree Lilacs located on the northern edge of the area hydrologically connected to RG-6, which would likely have accumulated at the RG-5 site just north of RG-6 or have been blown out of the area hydrologically connected to both sites by the dominant northwesterly and southeasterly winds.

Empirical data is lacking in relation to the influence of fragmentation in anthropogenic-induced landscapes on wind-driven dispersal (Chen et al., 2020) and precise local wind data was not collected at either RG-2 or RG-6 during the 2021 sampling season, but a detailed plant identification analysis of the samples collected from RG-5 and RG-6 throughout 2021 could offer additional insights into the influence of fragmentation and local wind patterns on gross solids transportation in residential areas.

The data analyses and interpretation of this study were limited by several methodological issues. The loss of several of the 2021 samples - due to contamination (grease dumps at RG-2), sampler failure (mesh sampler bags fell off sampler devices before collection), or lost samples - prevented a full comparison of both sites across all 18 sampling dates. Without records of all trees on privately owned property near RG-6 within the surrounding residential neighborhood, the nearest instance of an identified tree species may have been recorded at a greater distance than is accurate and the associated angles would therefore also be inaccurate, thus affecting the results depicted in Figure 5 and Figure 6. The effort to identify all of these trees was beyond the scope of this study. At RG-6, approximately 100-200 trees visible from the aerial map (Figure 2) were not included in the data analysis due to their distance from the rain garden, their lack of inclusion within the City of Saint Paul's boulevard tree planting data, and/or their location on private property. At RG-2, approximately 50 trees visible from the aerial map (Figure 1) were not included in the data analysis due to their distance from the rain garden or their lack of inclusion within the FM Landcare data. Cumulative precipitation data for RG-6 was also unavailable from the University of Minnesota's Saint Paul Campus Climate Observatory for the sampling period leading up to 4/7/2021 and 6/23/2021. The 2021 samples from RG-2 were not oven-dried before being weighed, inflating the recorded mass for those samples and preventing a

direct dry mass comparison of both sites, and a more specified particle size distribution analysis was not conducted for those samples. The paper bags used for oven-drying the RG-6 samples absorbed atmospheric moisture content quickly, likely contributing to subtle errors in measurements for small masses even after oven-drying and desiccation. The use of metal tins or glassware is recommended for future dry mass procedures.

There are multiple confounding variables that may have influenced the measured prevalence of wind-driven and water-driven modes of transportation in this study. These confounding variables are unlikely to explain all of the material classified as wind-driven at either of the sites used in this study, but future studies should attempt to account for them. Human-driven transportation of plant material, through vehicle traffic on roadways at both sites and in the parking lots near RG-2 (affecting local winds and potentially depositing plant material carried from distant locations), and land and yard maintenance (leaf blowing, raking, tree pruning) at both sites, may have increased the prevalence of identified material with nearest instances outside of the areas hydrologically connected to the rain gardens, potentially artificially inflating the measured prevalence of wind-driven transportation.

The use of the nearest instances of each species and the assumption that instances of species within the areas hydrologically connected to the rain gardens were the parent trees of the identified material from those species were ideal ways for possible mechanisms behind their deposition to be measured in this study as they resulted in conservative estimates with preference for water-driven transport for which evidence has already been documented. However, these assumptions may have reduced the measured prevalence of wind-driven transportation as a result, primarily at RG-6 where several of the species within the hydrologically connected area had additional instances outside of the hydrologically connected area that were closer to the rain

garden, as well as reduced the estimated maximum distance traveled by plant material at both sites. The use of mass as a measurement of the prevalence of different species at each site also presents limitations. The average mass of senescent leaves just prior to abscission differs by species, as do the masses of other plant parts such as seeds, flowers, and fruits. For example, the average mass of a needle cluster from a Red Pine (*Pinus resinosa*) will be much smaller than that of a Red Maple (*Acer rubrum*) leaf, and an abundance of Red Pine needle clusters compared to only a few Red Maple leaves would not be conveyed through their mass measurements alone. Counting the individual number of plant parts identified from each species may offer a more accurate measurement of their prevalence.

The size, shape, and weight of plant parts from each species affect their terminal velocities, how far they are likely to fall from their parent tree, and how readily they can be transported by wind, with deciduous leaves being more aerodynamic than coniferous needles, terminal velocity being inversely correlated with dispersal ability, and leaves with lower weights and surface areas tending to travel farther than those with higher weights and surface areas (Ferguson, 1985; France, 1985; Greene and Johnson, 1993; Molnár et al., 2004). The height at which plant parts are released is positively correlated with their dispersal ability (Travis et al., 2010; Thomson et al., 2011), suggesting that the height of trees, the size of their canopy cover, and the type of surfaces (bare ground, ground with vegetation cover, or impervious surfaces) onto which individual plant parts fall can all influence their susceptibility to wind-driven transportation. Additionally, humidity levels and species and plant-part-specific moisture content will affect their weights (Ferguson, 1985). This is supported by findings from both sites (Figure 4a, 4b, and 4c) as decreases in the amount of cumulative precipitation between sampling dates generally correlated with increases in the mass of identified material from species outside the

hydrologically connected area, and increases in cumulative precipitation between sampling dates generally correlated with increases in the mass of identified material from species with instances within the areas hydrologically connected to each rain garden, suggesting that plant material was more susceptible to wind-driven transportation once excess moisture from precipitation events had evaporated. The amount of leachable P also differs across species and individual plant parts, with Silver Maple (*Acer saccharinum*) and Green Ash (*Fraxinus pennsylvanica*) leaves having more leachable P than Norway Maple (*Acer platanoides*) and Northern Pin Oak leaves (*Quercus ellipsoidalis*), Honey Locust (*Gleditsia triacanthos*) leaves having more than all of them, and leaves generally having more leachable P than seeds because seeds are designed to preserve their nutrients for germination (Dorney, 1986; Hobbie et al., 2016; Selbig, 2016).

Canopy cover, while influencing the amount of plant material produced (Hobie et al., 2015; Winston et al., 2023), has been shown to impact precipitation throughfall, with leaf type, phenological periods, and rainfall depth having significant influences on throughfall rates (Beidokhti and Moore, 2021). This suggests that the amount and type of canopy cover over streets influences runoff volumes during precipitation events and can impact the prevalence of water-driven transportation of gross solids as well as stormwater nutrient concentrations (Janke et al., 2017). Additionally, phenological trends differ by species (Molnár et al., 2004) and are impacted by geography and climate (Janke et al., 2017) such that seasonal litterfall trends may differ based on annual climate, and seasonal street sweeping programs designed to address bi-annual periods of peak litterfall may miss opportunities to reduce P contributions from species with phenological trends that do not align with the majority. Species-specific phenological trends should be considered for boulevard tree plantings to reduce P contributions to stormwater during seasons when street sweeping programs are not active (Duan et al., 2014). Furthermore, more

research is needed to understand the role of litterfall into yards and to guide outreach to private residences to reduce additional partially-human-driven transportation of material due to management practices.

An experimental approach to assessing the influence of wind-driven and water-driven transportation on gross solids would need to account for human-driven transportation, variation in species-specific and plant-part-specific mass and aerodynamics, and definitive location of origin for identified species. An ideal method to achieve this goal could include the use of artificial trees, each constructed identically and with the same predetermined number of artificial leaves attached. Artificial leaves could be made from different colors of construction paper to represent different species, all cut to the same dimensions. The artificial leaves could be attached to the artificial trees using an automated controlled release mechanism or through the use of a biodegradable adhesive material that would begin to release the leaves from the tree after a predetermined amount of time. The trees could be placed in an outdoor area with a catchment basin and well-understood hydrologic connections, free of human traffic and any structures that would cause local wind fragmentation or reduce the influence of precipitation, and large enough to accommodate multiple artificial trees both within and outside of the area hydrologically connected to the catchment basin. Local wind and precipitation data could be collected on-site throughout the duration of the experiment. Artificial leaves that accumulate within the catchment basin could be collected and counted multiple times throughout the experiment, their colors identifying the location of their artificial trees of origin and whether or not they were transported to the catchment basin via wind-driven or water-driven transportation. Subsequent experiments could assess the influence of additional variables on transportation mechanics, such as the shapes

and sizes of the artificial leaves, the heights of the artificial trees, and their orientations in relation to the dominant directions of local wind.

For the expansion of the current dataset, a detailed size particle distribution is suggested for the 2021 samples collected from RG-2 to allow for a comparison with the data from RG-6, allowing for the assessment of differences between particle size distributions of stormwater solids collected within a light commercial area and a residential area. A detailed plant identification and particle size distribution analysis of the samples collected from RG-5 and RG-6 throughout 2021, along with a comparison of their ranges of cumulative mass of identified species based on angles of their nearest instance from the respective rain garden overlaid on the same cumulative wind data from Figure 4, could reveal additional insights into the influence of fragmentation and local wind patterns on gross solids transportation in residential areas. Additionally, detailed plant identification and particle size distribution analysis of the samples collected from all five sites throughout the 2022 sampling season could offer the opportunity to further assess the relationships between wind and precipitation trends and the prevalence of wind-driven and water-driven modes of gross solids transportation, as well as the influence of land use on the particle size distributions of stormwater solids samples. It is recommended that more complete tree planting data be obtained in advance of such analyses. The tree species with the most distant nearest instance to show up in the samples was the Japanese Elm tree, located over 295 meters from the RG-2 catchment basin. A suggested minimum radius from each rain garden site within which tree planting information should be obtained is 450 meters (approximately 1.5 times the distance from RG-2 to the nearest instance of Japanese Elm), and extra care should be taken to identify species along wind corridors and preferential wind directions.

5. Conclusion

In urban watersheds, gross solids materials have been shown to contribute significant amounts of P to stormwater runoff. Positive correlations have been identified between precipitation patterns and influxes of gross solids to stormwater runoff, but the role of wind-driven transportation as a contributor of organic material to urban stormwater solids remains poorly understood in comparison. A detailed analysis was conducted on identifiable tree material from gross solids samples captured at two different rain garden sites in the Minneapolis-Saint Paul metropolitan region to assess the possible mechanisms behind their deposition into the rain garden sites. It was assumed that material from outside of the watershed was transported by wind. Findings showed that material from outside the hydrologic watershed plays a significant role in the prevalence of gross solids, with an average percentage of 29% of material from outside the watershed and 71% from inside the watershed. Material from outside the watershed represented the majority of identified material from the residential street site. Material from within the watershed appeared to rise and fall along with precipitation patterns while material from outside the watershed appeared to fluctuate opposite them, suggesting that material from outside the watershed is more dominant in dryer conditions. The data presented herein inform the relevance of wind-driven transport, in addition to water-driven transport, as a key mode of transportation driving the dispersal of gross solids and influencing their nutrient pollutant contributions to urban stormwater, and reveal the importance of further research into its impacts and the factors that influence them. Growing our understanding of the differences between water-driven and wind-driven transportation of gross solids could help to further reduce urban sources of stormwater nutrient pollution and improve watershed health.

Appendix A

Particle Size Distribution and Organic/Inorganic Fractionation

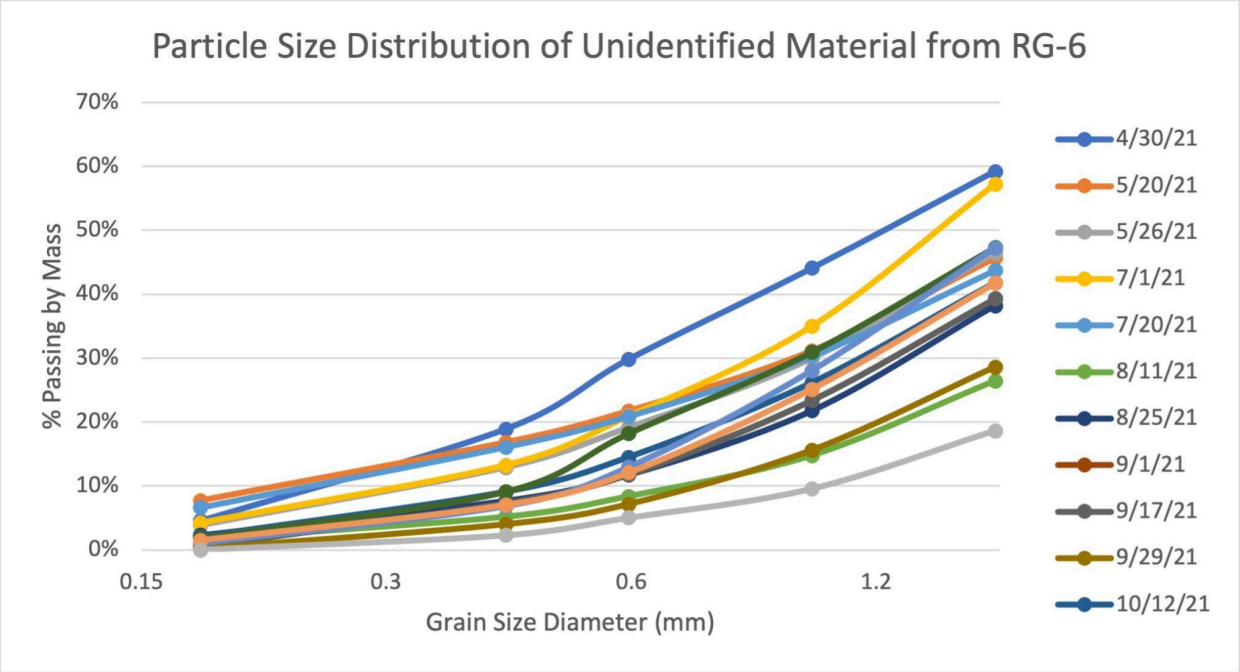

Figure A.1. Particle size distribution of unidentified material collected from RG-6 in 2021 by sampling date. The mass of particles was collected from mesh sizes of 1.68 mm, 1 mm, 0.595 mm, 0.42 mm, and 0.177 mm. The percent of the total mass of unidentified material that passed through each grain size is plotted on the y-axis and the grain size diameter is plotted in mm along the x-axis.

Table A.1. Particle size distribution data of unidentified material collected from RG-6 in 2021 by sampling date.

Particle Size Distribution of Unidentified Material from RG-6 (g)						
Sampling Date (MM/DD/YYYY)	**No. 12 (1.68 mm)**	**No. 18 (1 mm)**	**No. 30 (0.595 mm)**	**No. 40 (0.42 mm)**	**No. 80 (0.177 mm)**	**Bottom Pan**
4/30/21	40.32	14.96	14.09	10.77	14.19	4.5
5/20/21	76.51	20.47	13.28	6.94	12.82	10.82
5/26/21	14.5	4.48	2.93	1.69	2.45	1.04
7/1/21	20.91	10.88	6.87	3.74	4.41	2.07
7/20/21	22.77	5.41	3.83	1.94	3.83	2.67
8/11/21	127.42	20.19	11.07	5.54	6.2	2.78
8/25/21	66.21	17.63	10.75	4.34	5.77	2.45
9/1/21	137.11	35.73	29.21	14.62	22.74	11.64
9/17/21	17.32	4.54	3.31	1.28	1.94	0.14

9/29/21	48.37	8.82	5.73	2.13	2.59	0.12
10/12/21	34.53	9.27	6.9	3.21	4.16	1.23
10/26/21	0.29	0.09	0.07	0.05	0.04	0.01
11/9/21	3.46	1.26	0.99	0.4	0.38	0.07
11/17/21	1.16	0.33	0.26	0.1	0.11	0.03
12/1/21	1.79	0.2	0.1	0.06	0.05	0

Particle settling is a primary removal mechanism of nutrient pollutants from stormwater. Accordingly, particle size distributions (PSDs) are of critical importance when trying to understand the fate and transportation of sediments through stormwater control measures (Selbig, 2016). Land use has been found to influence median particle sizes, with parking lot sites having smaller median particle sizes than residential and commercial streets (Selbig and Bannerman, 2011). Accordingly, PSDs can be used to inform appropriate stormwater control measures and minimize contributions to the nutrient pollution of urban stormwater. A detailed PSD analysis is suggested for the samples collected at the RG-2 site in 2021 to allow for comparison with the PSD data from RG-6 (Figure A.1.).

a)

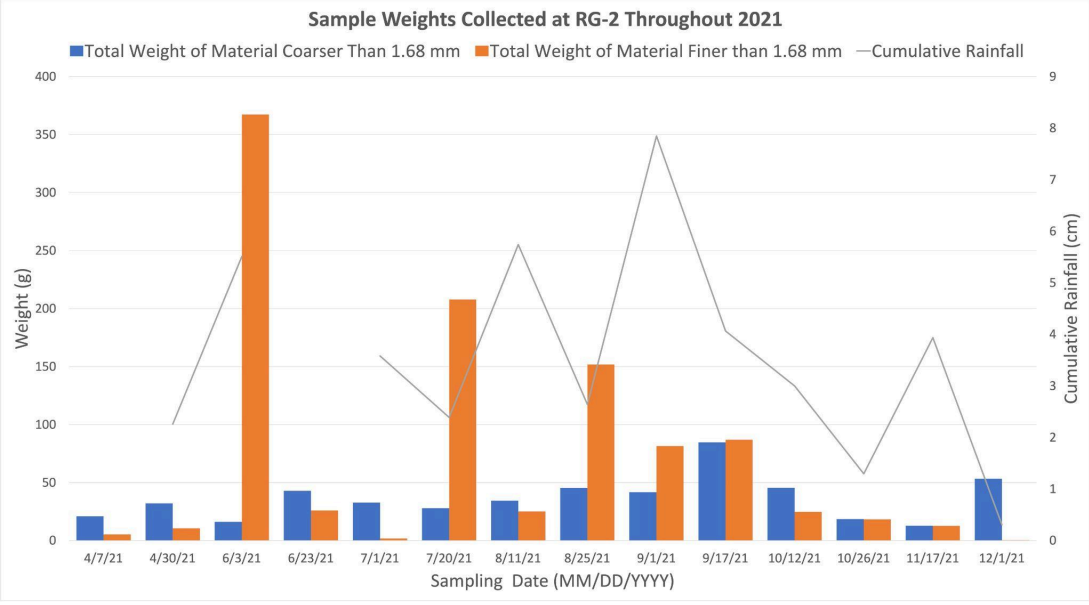

b)

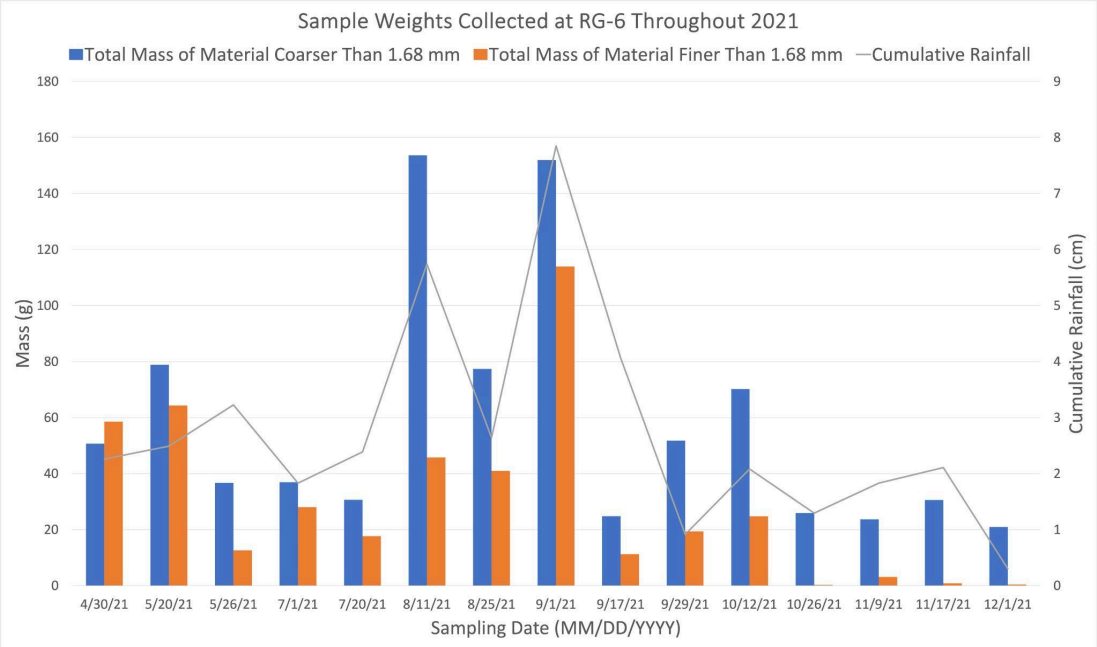

Figure A.2. The combined mass of material coarser than 1.68 mm compared to the combined mass of material finer than 1.68 mm at RG-2 (a) and RG-6 (b) by sampling date, with cumulative precipitation between sampling dates plotted on a secondary axis.

Appendix B

Species-Specific Phenology

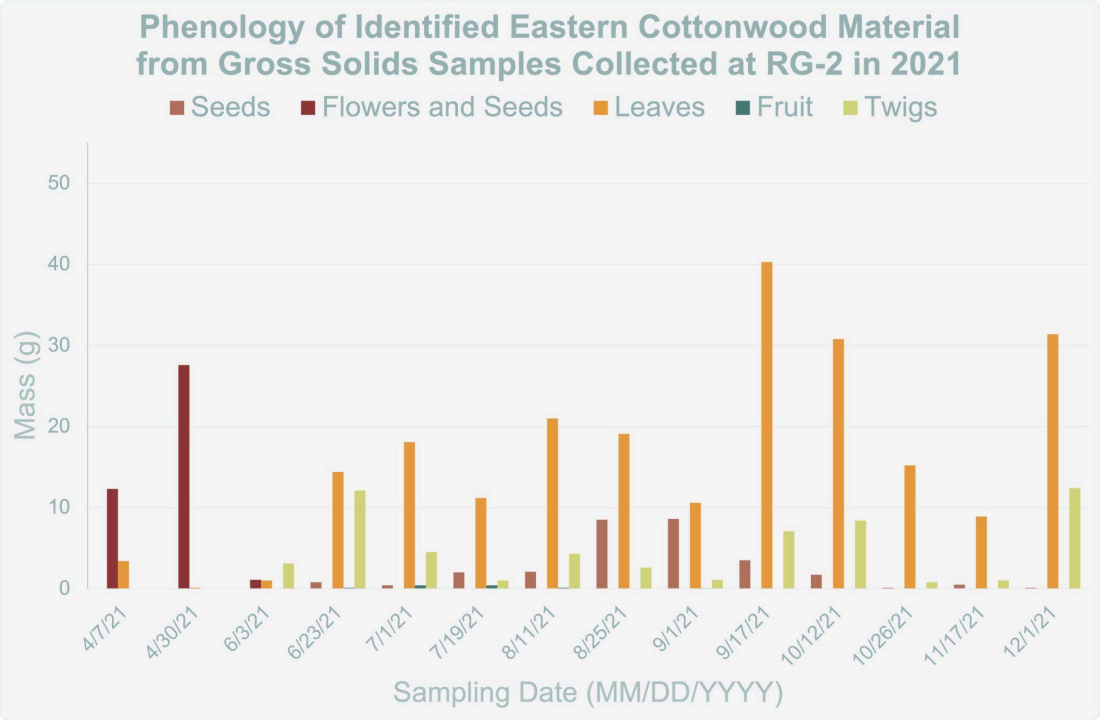

Figure B.1. The combined mass of identified Eastern Cottonwood (*Populus deltoides*) material, differentiated by plant part, collected at RG-2 and arranged by sampling date.

Table B.1. Phenology of identified Eastern Cottonwood (*Populus deltoides*) material from samples collected at RG-2 over the 2021 sampling season.

Phenology of Identified Eastern Cottonwood Material from Gross Solids Samples Collected at RG-2 in 2021					
Sampling Date	**Flowers and Seeds (g)**	**Seeds (g)**	**Leaves (g)**	**Fruit (g)**	**Twigs (g)**
4/7/21	12.3	0	3.4	0	0
4/30/21	27.6	0	0.1	0	0
6/3/21	1.1	0	1	0	3.1
6/23/21	0	0.8	14.4	0.1	12.1
7/1/21	0	0.4	18.1	0.4	4.5
7/19/21	0	2	11.2	0.4	1
8/11/21	0	2.1	21	0.1	4.3
8/25/21	0	8.5	19.1	0	2.6
9/1/21	0	8.6	10.6	0.05	1.1

9/17/21	0	3.5	40.3	0	7.1
10/12/21	0	1.7	30.8	0	8.4
10/26/21	0	0.1	15.2	0	0.8
11/17/21	0	0.5	8.9	0	1
12/1/21	0	0.1	31.4	0	12.4

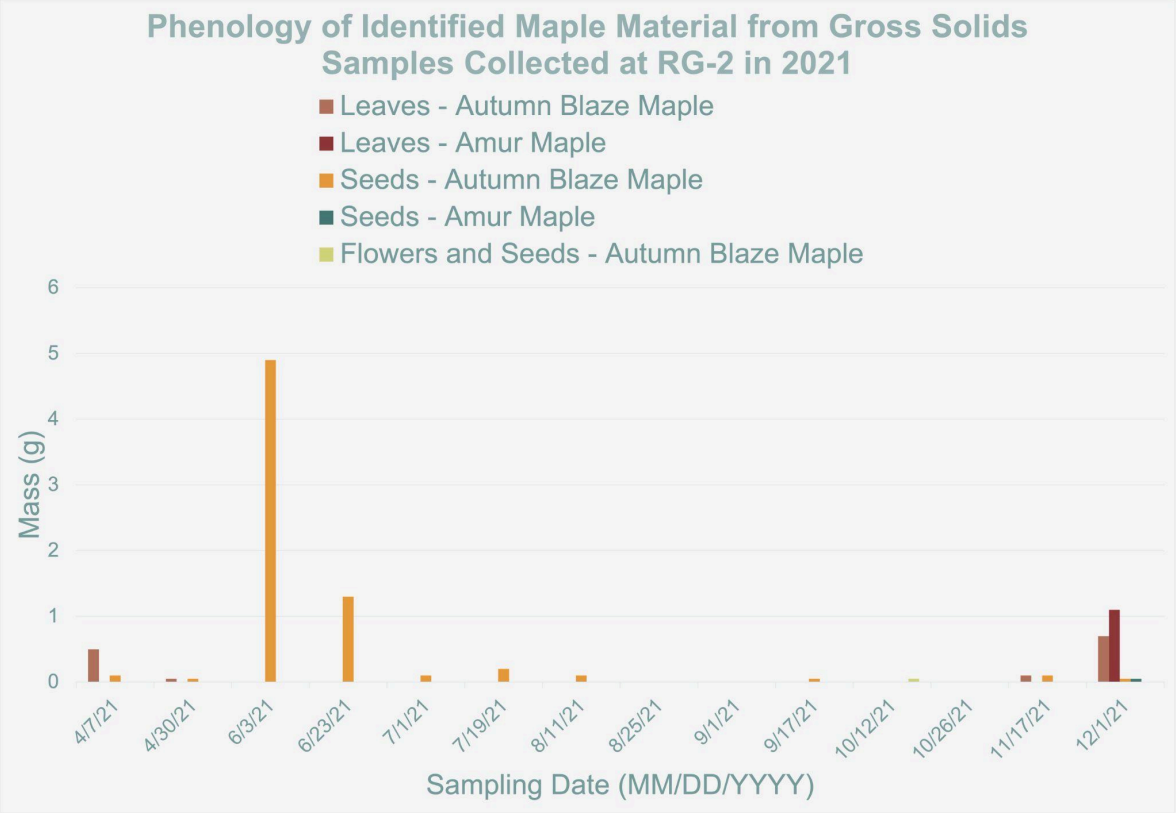

Figure B.2. The combined mass of identified Autumn Blaze Maple (*Acer freemanii*) and Amur Maple (*Acer ginnala*) material, differentiated by plant part and species, collected at RG-2 and arranged by sampling date.

Table B.2. Phenology of identified Autumn Blaze Maple (*Acer freemanii*) and Amur Maple (*Acer ginnala*) material from samples collected at RG-2 over the 2021 sampling season.

Phenology of Identified Maple Material from Gross Solids Samples Collected at RG-2 in 2021					
Sampling Date	**Leaves - Autumn Blaze Maple (g)**	**Leaves - Amur Maple (g)**	**Seeds - Autumn Blaze Maple (g)**	**Seeds - Amur Maple (g)**	**Flowers and Seeds - Autumn Blaze Maple (g)**
4/7/21	0.5	0	0.1	0	0
4/30/21	0.05	0	0.05	0	0
6/3/21	0	0	4.9	0	0

6/23/21	0	0	1.3	0	0
7/1/21	0	0	0.1	0	0
7/19/21	0	0	0.2	0	0
8/11/21	0	0	0.1	0	0
8/25/21	0	0	0	0	0
9/1/21	0	0	0	0	0
9/17/21	0	0	0.05	0	0
10/12/21	0	0	0	0	0.05
10/26/21	0	0	0	0	0
11/17/21	0.1	0	0.1	0	0
12/1/21	0.7	1.1	0.05	0.05	0

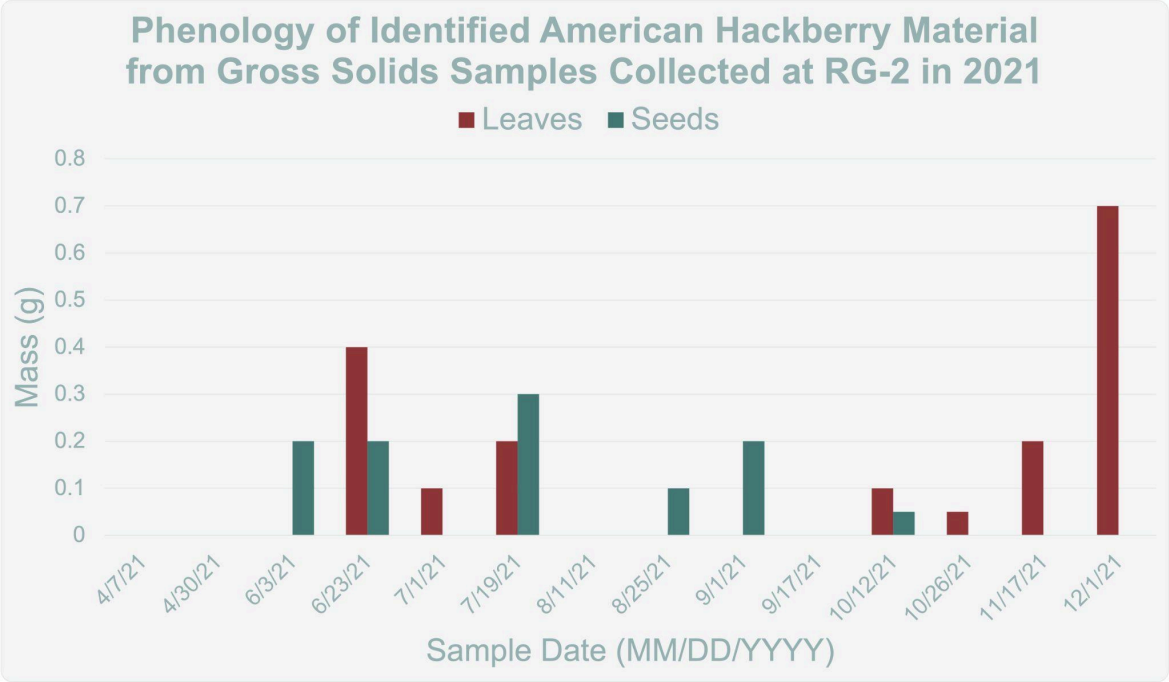

Figure B.3. The combined mass of identified American Hackberry (*Celtis occidentalis*) material, differentiated by plant part, collected at RG-2 and arranged by sampling date.

Table B.3. Phenology of identified American Hackberry (*Celtis occidentalis*) material from samples collected at RG-2 over the 2021 sampling season.

Phenology of Identified American Hackberry Material from Gross Solids Samples Collected at RG-2 in 2021		
Sampling Date	**Leaves (g)**	**Seeds (g)**
4/7/21	0	0
4/30/21	0	0
6/3/21	0	0.2
6/23/21	0.4	0.2
7/1/21	0.1	0
7/19/21	0.2	0.3
8/11/21	0	0
8/25/21	0	0.1
9/1/21	0	0.2
9/17/21	0	0
10/12/21	0.1	0.05
10/26/21	0.05	0
11/17/21	0.2	0
12/1/21	0.7	0

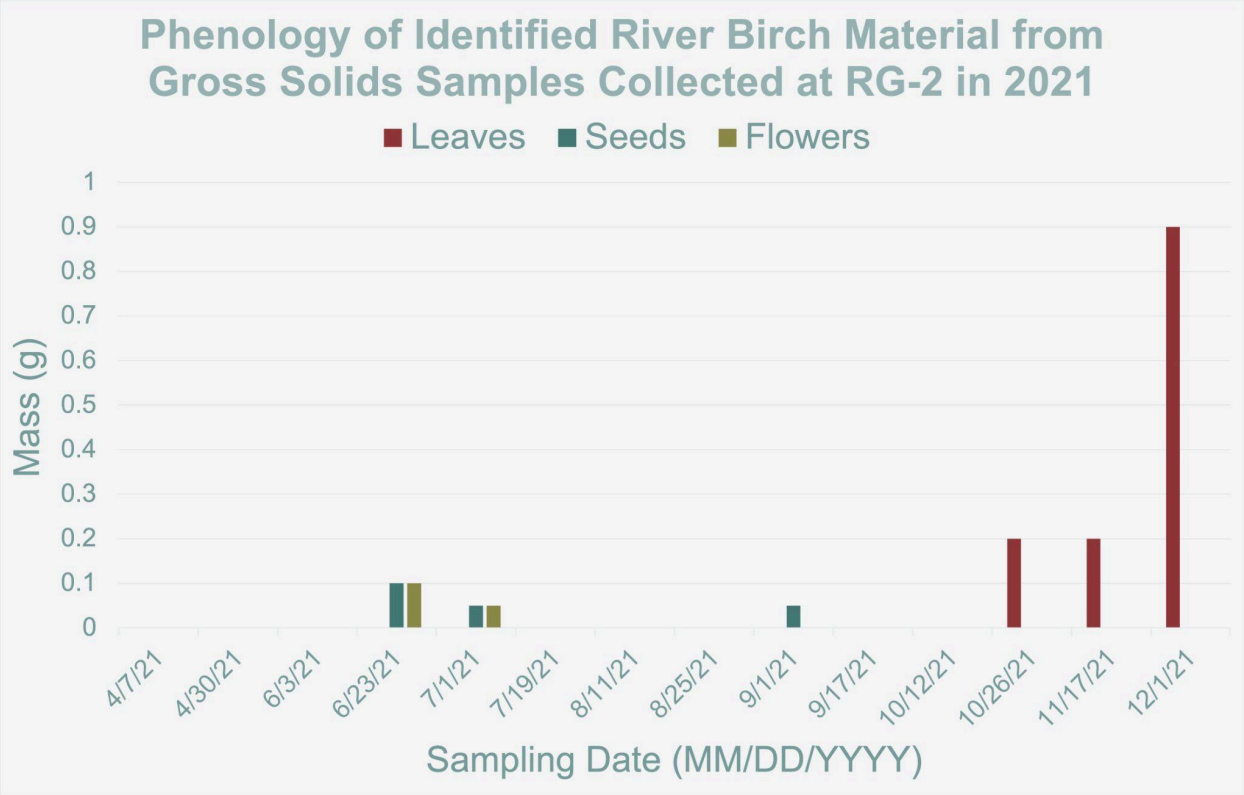

Figure B.4. The combined mass of identified River Birch (*Betula nigra*) material, differentiated by plant part, collected at RG-2 and arranged by sampling date.

Table B.4. Phenology of identified River Birch (*Betula nigra*) material from samples collected at RG-2 over the 2021 sampling season.

Phenology of Identified River Birch Material from Gross Solids Samples Collected at RG-2 in 2021			
Sampling Date	**Leaves (g)**	**Seeds (g)**	**Flowers (g)**
4/7/21	0	0	0
4/30/21	0	0	0
6/3/21	0	0	0
6/23/21	0	0.1	0.1
7/1/21	0	0.05	0.05
7/19/21	0	0	0
8/11/21	0	0	0
8/25/21	0	0	0

9/1/21	0	0.05	0
9/17/21	0	0	0
10/12/21	0	0	0
10/26/21	0.2	0	0
11/17/21	0.2	0	0
12/1/21	0.9	0	0

Phenological trends differ by species (Molnár et al., 2004) and are impacted by geography and climate (Janke et al., 2017) such that seasonal litterfall trends may differ based on annual climate, and seasonal street sweeping programs designed to address bi-annual periods of peak litterfall may miss opportunities to reduce P contributions from species with phenological trends that do not align with the majority. Species-specific phenological trends should be considered for boulevard tree plantings to reduce P contributions to stormwater during seasons when street sweeping programs are not active (Duan et al., 2014). Figures B.1., B.2., B.3., and B.4. represent phenological trends of material from five different tree species identified within the samples collected from RG-2 in 2021.

Appendix C

Specified Analysis of Dominant Wind Direction, Wind Speed, and Precipitation

Upon closer inspection of Figure 4, it appears that there may be an approximate one-week delay between when the cumulative precipitation measurements for sampling dates from 2021 were collected and when their effects can be seen within the identified gross solids material in the form of fluctuations in water-driven and wind-driven transportation. A more detailed analysis of the precipitation data between sampling events could reveal a stronger relationship between the timing and intensity of rain events and the accompanying changes in gross solids transportation that follow. An analysis of cumulative wind and precipitation data between each sampling period may reveal additional trends with the mass of gross solids collected at each site.

Table C.1. Angle from the RG-2 catchment basin to the trunk of the nearest instance of each tree species.

Angle to Nearest Instance of Tree Species at the Ski-U-Mah Parking Lot Rain Garden Site (RG-2) in 2021	
Tree Species Common Name (*Scientific Name*)	**Angle to Nearest Instance (°)**
American Hackberry *(Celtis occidentalis)*	*276.84*
American Hornbeam *(Carpinus caroliniana)*	*104.25*
Amur Maple *(Acer ginnala)*	*215.91*
Autumn Blaze Maple *(Acer freemanii)*	*237.47*
Bur Oak *(Quercus macrocarpa)*	*75.17*
Crabapple *(Malus)*	*125.33*
Dawn Redwood *(Metasequoia)*	*132.78*
Eastern Cottonwood* *(Populus deltoides)*	*326.55*
Ginko *(Ginkgo biloba)*	*262.59*
Green Ash *(Fraxinus pennsylvanica)*	*61.30*
Japanese Elm *(Ulmus davidiana var. japonica)*	*305.80*

River Birch *(Betula nigra)*	*228.32*
Swamp White Oak *(Quercus bicolor)*	*272.47*
** Denotes species with instances within the area hydrologically connected to the rain garden*	

Table C.2. Angle from the RG-6 catchment basin to the trunk of the nearest instance of each tree species.

Angle to Nearest Instance of Tree Species at the Pascal Center Rain Garden Site (RG-6) in 2021	
Tree Species Common Name (*Scientific Name*)	**Angle to Nearest Instance (°)**
Accolade Elm *(Ulmus 'Morton')*	*346.80*
American Elm *(Ulmus americana)*	*192.82*
American Hackberry* *(Celtis occidentalis)*	*5.46*
American Hornbeam* *(Carpinus caroliniana)*	*22.69*
American Linden *(Tilia americana)*	*357.12*
Autumn Blaze Maple *(Acer freemanii)*	*340.42*
Autumn Blaze White Ash *(Fraxinus americana 'Autumn Blaze')*	*355.32*
Black Maple *(Acer nigrum)*	*325.75*
Blue Spruce *(Picea pungens)*	*302.32*
Crabapple *(Malus)*	*342.49*
Dawn Redwood *(Metasequoia)*	*306.47*
Eastern Cottonwood *(Populus deltoides)*	*155.31*
Frontier Elm *(Ulmus 'Frontier')*	*2.12*
Green Ash *(Fraxinus pennsylvanica)*	*175.25*
Honey Locust *(Gleditsia triacanthos)*	*6.77*
Japanese Tree Lilac* *(Syringa reticulata)*	*6.81*
Kentucky Coffeetree *(Gymnocladus dioicus)*	*349.11*
Kentucky Coffeetree Espresso *(Gymnocladus dioicus 'Espresso')*	*356.30*
London Planetree *(Platanus × acerifolia)*	*286.51*
New Harmony American Elm *(Ulmus americana 'New Harmony')*	*176.43*

Northern Pin Oak *(Quercus ellipsoidalis)*	*133.32*
Northern Red Oak* *(Quercus rubra)*	*3.86*
Norway Maple* *(Acer platanoides)*	*8.16*
Norway Spruce *(Picea abies)*	*344.28*
Red Maple *(Acer rubrum)*	*356.47*
Red Pine *(Pinus resinosa)*	*153.36*
River Birch *(Betula nigra)*	*357.60*
Scotch Pine *(Pinus sylvestris)*	*168.77*
Silver Maple* *(Acer saccharinum)*	*12.33*
Triumph Elm *(Ulmus 'Morton Glossy')*	*1.93*
White Ash *(Fraxinus americana)*	*1.39*
White Mulberry *(Morus alba)*	*138.93*
White Pine *(Pinus strobus)*	*132.04*
White Poplar *(Populus alba)*	*156.69*
White Spruce *(Picea glauca)*	*53.62*
Yellow Birch *(Betula alleghaniensis)*	*81.88*

** Denotes species with instances within the area hydrologically connected to the rain garden*

References

Allison, R. A.; Chiew, F. H. S.; McMahon, T. A. Nutrient Contribution of Leaf Litter in Urban Stormwater. *Journal of Environmental Management* **1998**, *54* (4), 269–272. https://doi.org/10.1006/jema.1998.0334.

Chen, S.-C.; Dener, E.; Altman, A.; Chen, F.; Giladi, I. Effect of Habitat Fragmentation on Seed Dispersal Ability of a Wind-Dispersed Annual in an Agroecosystem. *Agriculture, ecosystems & environment* **2020**, *304*, 107138-. https://doi.org/10.1016/j.agee.2020.107138.

Chowdhury, A.; Egodawatta, P.; McGree, J. Pattern-Based Assessment of the Influence of Rainfall Characteristics on Urban Stormwater Quality. *Water science and technology : a journal of the International Association on Water Pollution Research.* **2023**, *87* (9), 2292–2303. https://doi.org/10.2166/wst.2023.125.

Correll, D. L. The Role of Phosphorus in the Eutrophication of Receiving Waters; a Review. *Journal of Environmental Quality* **1998**, *27* (2), 261–266. https://doi.org/10.2134/jeq1998.00472425002700020004x.

Damschen, E. I.; Baker, D. V.; Bohrer, G.; Nathan, R.; Orrock, J. L.; Turner, J. R.; Brudvig, L. A.; Haddad, N. M.; Levey, D. J.; Tewksbury, J. J. How Fragmentation and Corridors Affect Wind Dynamics and Seed Dispersal in Open Habitats. *Proceedings of the National Academy of Sciences - PNAS* **2014**, *111* (9), 3484–3489. https://doi.org/10.1073/pnas.1308968111.

Dirr, M. *Manual of Woody Landscape Plants : Their Identification, Ornamental Characteristics, Culture, Propagation, and Uses*, 6th ed.; Stipes Pub.: Champaign, Ill, **2009**.

Dorney, J. R. Leachable and Total Phosphorus in Urban Street Tree Leaves. *Water, air, and soil pollution* **1986**, *28* (3–4), 439–443. https://doi.org/10.1007/BF00583506.

Duan, S.; Delaney-Newcomb, K.; Kaushal, S. S.; Findlay, S. E. G.; Belt, K. T. Potential Effects of Leaf Litter on Water Quality in Urban Watersheds. *Biogeochemistry* **2014**, *121* (1), 61–80. https://doi.org/10.1007/s10533-014-0016-9.

Ferguson, D. K. Plant Part Processing and Community Reconstruction. *Eclogae geologicae Helvetiae* **1995**, *88* (3), 627–641.

Ferguson, D. K. The Origin of Leaf-Assemblages; New Light on an Old Problem. *Review of paleobotany and palynology* **1985**, *46* (1–2), 117–118. https://doi.org/10.1016/0034-6667(85)90041-7.

FM Landcare - Trees by Type. *Map Viewer*. umn-egis.maps.arcgis.com. https://umn-egis.maps.arcgis.com/apps/mapviewer/index.html?webmap=c5aeffa74e1844b5b68e201eda933375 (accessed 2023-11-24).

France, R. L. Empirically Estimating the Lateral Transport of Riparian Leaf Litter to Lakes. *Freshwater Biology* **1995**, *34* (3), 495–499. https://doi.org/10.1111/j.1365-2427.1995.tb00907.x.

Greene, D. F.; Johnson, E. A. Seed Mass and Dispersal Capacity in Wind-Dispersed Diaspores. *Oikos* **1993**, *67* (1), 69–74. https://doi.org/10.2307/3545096.

Herzmann, Daryl. "Iowa Environmental Mesonet: Custom Wind Roses." *Mesonet.agron.iastate.edu*, Iowa State University, **2023**, www.mesonet.agron.iastate.edu/sites/dyn_windrose.phtml?station=STP&network=MN_ASOS. Accessed 25 Nov. 2023.

Hobbie, S. E.; Baker, L. A.; Buyarski, C.; Nidzgorski, D.; Finlay, J. C. Decomposition of Tree Leaf Litter on Pavement: Implications for Urban Water Quality. *Urban Ecosystems* **2014**, *17* (2), 369–385. https://doi.org/10.1007/s11252-013-0329-9.

Hobbie, S. E.; Finlay, J. C.; Janke, B. D.; Nidzgorski, D. A.; Millet, D. B.; Baker, L. A. Contrasting Nitrogen and Phosphorus Budgets in Urban Watersheds and Implications for Managing Urban Water Pollution. *Proceedings of the National Academy of Sciences - PNAS* **2017**, *114* (16), 4177–4182. https://doi.org/10.1073/pnas.1618536114.

Hobbie, S. E.; King, R.; Belo, T.; Baker, L. A.; Finlay, J. C. *Developing a Street Sweeping Credit for Stormwater Phosphorus Source Reduction: Final Report*; **2020**.

Janke, B. D.; Finlay, J. C.; Hobbie, S. E. Trees and Streets as Drivers of Urban Stormwater Nutrient Pollution. *Environmental science & technology* **2017**, *51* (17), 9569–9579. https://doi.org/10.1021/acs.est.7b02225.

Janke, B. D.; Finlay, J. C.; Taguchi, V. J.; Gulliver, J. S. Hydrologic Processes Regulate Nutrient Retention in Stormwater Detention Ponds. *The Science of the total environment* **2022**, *823*, 153722–153722. https://doi.org/10.1016/j.scitotenv.2022.153722.

Kalinosky, P., L. Baker, S. Hobbie, R. Bintner. *User Support Manual: Estimating Nutrient Removal by Enhanced Street Sweeping*; **2014**.

Li, Y.; Lau, S.-L.; Kayhanian, M.; Stenstrom, M. K. Particle Size Distribution in Highway Runoff. *Journal of environmental engineering (New York, N.Y.)* **2005**, *131* (9), 1267–1276. https://doi.org/10.1061/(ASCE)0733-9372(2005)131:9(1267).

Ma, J.; Ying, G.; Sansalone, J. J. Transport and Distribution of Particulate Matter Phosphorus Fractions in Rainfall-Runoff from Roadway Source Areas. *Journal of environmental*

engineering (New York, N.Y.) **2010**, *136* (11), 1197–1205. https://doi.org/10.1061/(ASCE)EE.1943-7870.0000263.

Mathooko, J. M.; Morara, G. O.; Leichtfried, M. Leaf Litter Transport and Retention in a Tropical Rift Valley Stream: An Experimental Approach. *Hydrobiologia* **2001**, *443* (1–3), 9–18. https://doi.org/10.1023/A:1017542617696.

Molnár, J.; Erdei B.; Hably L. The transport of leaves and fruits - a taphonomical study of leaf litter. *Annales historico-naturales Musei Nationalis Hungarici* **2004**, *96,* 29-50.

Nooraei Beidokhti, A.; Moore, T. L. The Effects of Precipitation, Tree Phenology, Leaf Area Index, and Bark Characteristics on Throughfall Rates by Urban Trees: A Meta-Data Analysis. *Urban forestry & urban greening* **2021**, *60*, 127052-. https://doi.org/10.1016/j.ufug.2021.127052.

Pietsch, A. Accumulation, Nutrient Content, and Settling Rates of Coarse Organic Solids in Minnesota Stormwater, **2022**.

Rio, M.; Salles, C.; Tournoud, M.-G. Modeling the Effects of Stormwater Control Measures on Runoff Volume and Particulate Load in Urban Catchments. *Urban water journal.* **2021**, *18* (2), 79–90. https://doi.org/10.1080/1573062X.2020.1860236.

Sauer, T. J.; Cambardella, C. A.; Brandle, J. R. Soil Carbon and Tree Litter Dynamics in a Red Cedar-Scotch Pine Shelterbelt. *Agroforestry Systems* **2007**, *71* (3), 163–174. https://doi.org/10.1007/s10457-007-9072-7.

Schindler, D. W.; Carpenter, S. R.; Chapra, S. C.; Hecky, R. E.; Orihel, D. M. Reducing Phosphorus to Curb Lake Eutrophication Is a Success. *Environmental science & technology* **2016**, *50* (17), 8923–8929. https://doi.org/10.1021/acs.est.6b02204.

Selbig, W. R.; Bannerman, R. T. *Characterizing the Size Distribution of Particles in Urban Stormwater by Use of Fixed-Point Sample-Collection Methods*; U.S. Dept. of the Interior, U.S. Geological Survey: Reston, Va, **2011**.

Selbig, W. R. Evaluation of Leaf Removal as a Means to Reduce Nutrient Concentrations and Loads in Urban Stormwater. *The Science of the total environment* **2016**, *571*, 124–133. https://doi.org/10.1016/j.scitotenv.2016.07.003.

Settle, S.; Goonetilleke, A.; Ayoko, G. A. Determination of Surrogate Indicators for Phosphorus and Solids in Urban Stormwater: Application of Multivariate Data Analysis Techniques. *Water, air, and soil pollution.* **2007**, *182* (1–4), 149–161. https://doi.org/10.1007/s11270-006-9328-2.

Standard Test Methods for Particle-Size Distribution (Gradation) of Soils Using Sieve Analysis. West Conshohocken, PA, ASTM International, **2017**, compass.astm.org/document/?contentCode=ASTM%7CD6913_D6913M-17%7Cen-US&proxycl=https%3A%2F%2Fsecure.astm.org&fromLogin=true. Accessed 26 Nov. 2023.

Steinke, K.; Kussow, W. R.; Stier, J. C. Potential Contributions of Mature Prairie and Turfgrass to Phosphorus in Urban Runoff. *Journal of Environmental Quality* **2013**, *42* (4), 1176–1184. https://doi.org/10.2134/jeq2012.0494.

Thomson, F. J.; Moles, A. T.; Auld, T. D.; Kingsford, R. T. Seed Dispersal Distance Is More Strongly Correlated with Plant Height than with Seed Mass. *The Journal of Ecology* **2011**, *99* (6), 1299–1307. https://doi.org/10.1111/j.1365-2745.2011.01867.x.

Travis, J. M. J.; Smith, H. S.; Ranwala, S. M. W. Towards a Mechanistic Understanding of Dispersal Evolution in Plants: Conservation Implications. *Diversity & distributions* **2010**, *16* (4), 690–702. https://doi.org/10.1111/j.1472-4642.2010.00674.x.

Waickowski, S. E. Gross Solids in Urban Catch Basins: A Pollutant Accounting Opportunity? **2015**.

Warneke, C. R.; Caughlin, T. T.; Damschen, E. I.; Haddad, N. M.; Levey, D. J.; Brudvig, L. A. Habitat Fragmentation Alters the Distance of Abiotic Seed Dispersal through Edge Effects and Direction of Dispersal. *Ecology (Durham)* **2022**, *103* (2), e03586-n/a. https://doi.org/10.1002/ecy.3586.

Watts, M. T. *Tree Finder : A Pocket Manual for Identification of Trees by Their Leaves*; Nature Study Guild: Place of publication not identified, **1963**.

Winston, R. J.; Hunt, W. F. Characterizing Runoff from Roads: Particle Size Distributions, Nutrients, and Gross Solids. *Journal of environmental engineering (New York, N.Y.)* **2017**, *143* (1). https://doi.org/10.1061/(ASCE)EE.1943-7870.0001148.

Winston, R. J.; Witter, J. D.; Tirpak, R. A.; Sester, L.; Jenkins, H.; Lillard, V. Abundance and Composition of Anthropogenic Macrolitter and Natural Debris in Road Runoff in Ohio, USA. *Water Research (Oxford)* **2023**, *239*, 120036–120036. https://doi.org/10.1016/j.watres.2023.120036.

Xiong, S. (Umea U.; Nilsson, C. Dynamics of Leaf Litter Accumulation and Its Effects on Riparian Vegetation: A Review. *The Botanical Review* **1997**, *63* (3), 240–264. https://doi.org/10.1007/BF02857951.

Yan, Y.; Xin, X.; Xu, X.; Wang, X.; Yan, R.; Murray, P. J. Vegetation Patches Increase Wind-Blown Litter Accumulation in a Semi-Arid Steppe of Northern China. *Environmental research letters* **2016**, *11* (12), 124008-. https://doi.org/10.1088/1748-9326/11/12/124008.

Yang, Y.-Y.; Toor, G. S. Sources and Mechanisms of Nitrate and Orthophosphate Transport in Urban Stormwater Runoff from Residential Catchments. *Water Research (Oxford)* **2017**, *112*, 176–184. https://doi.org/10.1016/j.watres.2017.01.039.

Zawilski, M. Assessment of Total Suspended Solid Emission Discharged *via* Storm Sewerage System from Urban Areas. *Ochrona środowiska.* **2013**, *35* (2), 33–40.

Zhang, Y.; Zhao, W.; Chen, X.; Jun, C.; Hao, J.; Tang, X.; Zhai, J. Assessment on the Effectiveness of Urban Stormwater Management. *Water.* **2021**, *13* (1). https://doi.org/10.3390/w13010004.